A peer-reviewed version of this preprint was published in PeerJ on 25 April 2016.

Doblin MA, Petrou K, Sinutok S, Seymour JR, Messer LF, Brown MV, Norman L, Everett JD, McInnes AS, Ralph PJ, Thompson PA, Hassler CS. 2016. Nutrient uplift in a cyclonic eddy increases diversity, primary productivity and iron demand of microbial communities relative to a western boundary current. PeerJ 4:e1973
https://doi.org/10.7717/peerj.1973

Nutrient uplift in a cyclonic eddy increases diversity, primary productivity and iron demand of microbial communities relative to a western boundary current

Martina A Doblin, Katherina Petrou, Sutinee Sinutok, Justin R Seymour, Lauren F Messer, Mark V Brown, Louiza Norman, Jason D Everett, Allison S McInnes, Peter J Ralph, Peter A Thompson, Christel S Hassler

The intensification of western boundary currents in the global ocean will potentially influence meso-scale eddy generation, and redistribute microbes and their associated ecological and biogeochemical functions. To understand eddy-induced changes in microbial community composition as well as how they control growth, we targeted the East Australian Current (EAC) region to sample microbes in a cyclonic (cold-core) eddy (CCE) and the adjacent EAC. Phototrophic and diazotrophic microbes were more diverse (2 to 10 times greater Shannon index) in the CCE relative to the EAC, and the cell size distribution in the CCE was dominated (67%) by larger micro-plankton (≥ 20 µm), as opposed to pico- and nano-sized cells in the EAC. Nutrient addition experiments determined that nitrogen was the principal nutrient limiting growth in the EAC, while iron was a secondary limiting nutrient in the CCE. Among the diazotrophic community, heterotrophic *NifH* gene sequences dominated in the EAC and were attributable to members of the gamma-, beta-, and delta-proteobacteria, while the CCE contained both phototrophic and heterotrophic diazotrophs, including *Trichodesmium*, UCYN-A and gamma-proteobacteria. Daily sampling of incubation bottles following nutrient amendment captured a cascade of effects at the cellular, population and community level, indicating taxon-specific differences in the speed of response of microbes to nutrient supply. Nitrogen addition to the CCE community increased picoeukaryote chlorophyll *a* quotas within 24 h, suggesting that nutrient uplift by eddies causes a 'greening' effect as well as an increase in phytoplankton biomass. After three days in both the EAC and CCE, diatoms increased in abundance with macronutrient (N, P, Si) and iron amendment , whereas haptophytes and phototrophic dinoflagellates declined. Our results indicate that cyclonic eddies increase delivery of nitrogen to the upper ocean to potentially mitigate the negative consequences of increased stratification due to ocean warming, but also increase the biological demand for iron that is necessary to sustain the growth of large-celled phototrophs and potentially support the diversity of diazotrophs over longer time-scales.

PeerJ Preprints | https://doi.org/10.7287/peerj.preprints.1854v1 | CC-BY 4.0 Open Access | rec: 12 Mar 2016, publ: 12 Mar 2016

Nutrient uplift in a cyclonic eddy increases diversity, primary productivity and iron demand of microbial communities relative to a western boundary current

M.A. Doblin[1], K. Petrou[2], S. Sinutok[1,3], J. Seymour[1], L.F. Messer[1], M.V. Brown[4], L. Norman[1,5], J.D. Everett[6], A. McInnes[1], P. J. Ralph[1], P.A. Thompson[7], C. Hassler[8]

1. Plant Functional Biology and Climate Change Cluster, University of Technology Sydney, Ultimo, NSW, Australia

2. School of Life Sciences, University of Technology Sydney, Ultimo, NSW, Australia

3. Faculty of Environmental Management, Prince of Songkla University, Kho Hong, Songkhla 90112, Thailand

4. School of Biotechnology and Biomolecular Sciences, University of New South Wales, Randwick, NSW, Australia

5. Department of Plant Sciences, University of Cambridge, Cambridge, United Kingdom

6. School of Biological, Earth and Environmental Sciences, University of New South Wales, Randwick, NSW, Australia

7. Oceans and Atmosphere Flagship, Commonwealth Scientific Industrial Research Organisation, , Hobart , Australia.

8. Institute F.-A. Forel, Earth and Environmental Sciences, University of Geneva, Geneva, Switzerland

Corresponding author:
Martina Doblin
Plant Functional Biology and Climate Change Cluster, University of Technology Sydney, Thomas Street, Ultimo, NSW, 2007, Australia
Martina.Doblin@uts.edu.au

Abstract

The intensification of western boundary currents in the global ocean will potentially influence meso-scale eddy generation, and redistribute microbes and their associated ecological and biogeochemical functions. To understand eddy-induced changes in microbial community composition as well as how they control growth, we targeted the East Australian Current (EAC) region to sample microbes in a cyclonic (cold-core) eddy (CCE) and the adjacent EAC. Phototrophic and diazotrophic microbes were more diverse (2 to 10 times greater Shannon index) in the CCE relative to the EAC, and the cell size distribution in the CCE was dominated (67%) by larger micro-plankton (≥ 20 μm), as opposed to pico- and nano-sized cells in the EAC. Nutrient addition experiments determined that nitrogen was the principal nutrient limiting growth in the EAC, while iron was a secondary limiting nutrient in the CCE. Among the diazotrophic community, heterotrophic *NifH* gene sequences dominated in the EAC and were attributable to members of the gamma-, beta-, and delta-proteobacteria, while the CCE contained both phototrophic and heterotrophic diazotrophs, including *Trichodesmium*, UCYN-A and gamma-proteobacteria. Daily sampling of incubation bottles following nutrient amendment captured a cascade of effects at the cellular, population and community level, indicating taxon-specific differences in the speed of response of microbes to nutrient supply. Nitrogen addition to the CCE community increased picoeukaryote chlorophyll *a* quotas within 24 h, suggesting that nutrient uplift by eddies causes a 'greening' effect as well as an increase in phytoplankton biomass. After three days in both the EAC and CCE, diatoms increased in abundance with macronutrient (N, P, Si) and iron amendment , whereas haptophytes and phototrophic dinoflagellates declined. Our results indicate that cyclonic eddies increase delivery of nitrogen to the upper ocean to potentially mitigate the negative consequences of increased stratification due to ocean warming, but also increase the biological demand for iron that is necessary to sustain

the growth of large-celled phototrophs and potentially support the diversity of diazotrophs over longer time-scales.

Introduction

There are two broad nutrient limitation regimes for phytoplankton growth in the contemporary ocean, whereby iron (Fe) limitation occurs across ~30% of the ocean's surface area where high macronutrient concentrations occur (high latitudes, upwelling and some coastal areas), and nitrogen (N) limitation occurs across most of the oligotrophic low-latitude systems (Moore et al. 2013). Different phytoplankton groups can have specific nutrient requirements, such as Fe for diazotrophs (Kustka et al 2003) and silicon (Si) for diatoms (Brzezinski & Nelson 1989), which may lead to secondary or interactive effects on Fe or N limitation. Co-limitation may also arise when there is physical mixing between water masses with different nutrient stoichiometry, or over seasonal cycles when physical nutrient inputs and biological cycling alters nutrient bioavailability (Deutsch & Weber 2012).

Global Climate Model (GCM) projections indicate warming and increased stratification of the upper ocean over the coming decades, limiting the upwards delivery of nitrogen (e.g., "new" N) into the euphotic zone, and potentially leading to increased reliance on a smaller pool of regenerated forms or N fixation to support primary production (Behrenfeld 2011). However, these models typically do not consider the influence of smaller scale oceanographic features such as meso-scale eddies, which could act as a compensatory mechanism and enrich the upper ocean with new nutrients delivered from deeper ocean waters, potentially mitigating the negative consequences of climate change (Matear et al. 2013).

While eddies are universal features of the global ocean (Chelton, Schlax & Samelson 2011), they differ in their mode of formation, direction of rotation, size, longevity, and processes driving nutrient dynamics (e.g. interaction between wind and surface currents, horizontal entrainment;

Gaube et al. 2014), and can thus have different biological effects (Bibby et al. 2008). Eddies formed in coastal regions, for example, can entrain enriched continental shelf water (Waite et al. 2007), and consequently have higher positive chlorophyll-a anomalies than their oceanic counterparts (Everett et al. 2012). The ratio of upwelled nutrients (e.g., Si:N) delivered into the euphotic zone is also important in determining the structure of microbial communities sustained by eddies and influences their biogeochemical function (Bibby & Moore 2011). Therefore, the role eddies play in regulating internal nutrient inputs from the deep ocean is likely to be regionally dependent.

Much of what is known about eddies and their impact on the base of the foodweb is derived from satellite ocean colour observations which provide limited information with respect to microbial species composition and biogeochemical activity, and have a restricted view of the upper ocean (McGillicuddy 2016). *In situ* observations and manipulative experiments are therefore critical to develop a full understanding of the role of meso-scale eddies in upper-ocean ecosystem dynamics and biogeochemical cycling.

Australia has one of the longest north-south coastlines in the world, and the oceanography along its east coast is extremely dynamic. It is strongly influenced by the flow of the Eastern Australian Current (EAC), one of five western boundary currents (WBCs) in the global ocean. Southward of ~32 °S 153 °E, where two thirds of the EAC deviates eastward towards New Zealand to form the Tasman Front, the remaining EAC flow meanders, breaking down into a complex series of meso-scale eddies (Ridgway & Godfrey, 1997). The number and frequency of these eddies is higher than in the broader Tasman Sea, and their biological properties differentiate more strongly from background ocean waters than their oceanic counterparts (Everett et al. 2014). A critical research question is whether the observed intensification of the EAC (Wu et al., 2012) will result in more

104 eddies, a change in the nature of these eddies, and how they will impact on primary producers
105 and higher trophic levels.

106 Given that offshore phytoplankton communities in the Tasman Sea are generally N limited
107 (Hassler et al. 2011; Ellwood et al. 2013), and that cyclonic cold-core eddies displace isopycnal
108 surfaces (seawater of similar density) upwards and can upwell nutrients into the euphotic zone
109 (McGillicuddy et al., 1998), EAC-induced eddies could increase the supply of nitrogen into
110 surface waters from below the thermocline and potentially alter controls on phytoplankton
111 growth. However, another source of N into surface waters is from N_2 fixing microbes. At least
112 four different groups of diazotrophs have been identified from Australian waters: the
113 filamentous, photosynthetic cyanobacterium *Trichodesmium*, the unicellular phycoerythrin-
114 containing cyanobacterium *Crocosphaera watsonii* (group B), the photoheterotrophic symbiont
115 UCYN-A (associated with specific prymnesiophyte hosts; Hagino et al. 2013), and heterotrophic
116 proteobacteria (Moisander et al. 2010; Seymour et al. 2012; Messer et al. 2015). The regional
117 distribution of diazotrophs in the western South Pacific suggests there is a sufficient supply of Fe
118 to satisfy the requirements of the nitrogenase enzyme (Kustka et al 2003), but little is known
119 about how eddies may change the delivery of Fe or N from depth in this region, and hence alter
120 the dynamics of diazotrophs relative to other microbial groups.

121 This study targeted the western Tasman Sea, which is dominated by the East Australian Current
122 (EAC) and its associated eddy field. We examined the composition and diversity of the microbial
123 community in a cyclonic cold core eddy (CCE) and in the EAC, and examined their responses to
124 separate additions of nitrate (N), nitrate with iron (NFe), silicic acid (Si) as well as a mix of
125 nutrients containing N, Fe, Si and phosphate (P). We focused on communities from the
126 subsurface chlorophyll-a maximum to simulate the impact of moderate nutrient uplift into the

euphotic zone (i.e., upwelling that does not reach the surface), and advance knowledge about responses of microbial communities that are difficult to detect using satellites.

Materials and Methods

Study site and water collection. The experiments were conducted on the *RV Southern Surveyor* during austral spring in 2010 (15 - 31 October) between 29 and 36 °S, and 150 and 155 °E (Fig. 1A). Sampling sites were chosen with the assistance of daily Moderate Resolution Imaging Spectroradiometer (MODIS) and Advanced Very High Resolution Radiometer (AVHRR) satellite imagery and targeted the EAC and a meso-scale cyclonic (cold core) eddy (CCE; Fig. 1B). To examine the oceanographic context of the sampling period, MODIS Level 3 sea-surface temperature was obtained from the Integrated Marine Observing System (IMOS) Data Portal (http://imos.aodn.org.au/imos/) at 1 km resolution. Satellite altimeter data were obtained from NASA/CNES (Jason-1 and 2) and ESA (ENVISAGE) via the IMOS portal.

At each site, the physico-chemical properties of the water column (0 – 200 m) were measured with the aid of a Conductivity-Temperature-Depth (CTD; Seabird SBE911-plus) equipped with a fluorometer (AquaTracker Mk3, Chelsea, UK), transmissometer (Wetlabs C-Star (25cm optical path)), dissolved oxygen (Seabird SBE43) and Photosynthetically Active Radiation (PAR; Biospherical Instruments QCP-2300 Log Quantum Cosine Irradiance Sensor) sensor.

Seawater used to assess microbial composition and diversity, as well as for nutrient amendment experiments was collected from the depth of the chlorophyll *a* (Chl-a) fluorescence maximum (as determined by the down-cast fluorescence profile) using 10 L Niskin bottles (80 m in the EAC, and 41 m in the CCE). A trace metal clean rosette was not available for this voyage, so the

following precautions were taken to minimise trace metal contamination. Water was sampled from Niskin bottles through acid washed silicon tubing with plastic bags covering the tubing and bottle neck, and polyethelene gloves were worn during water sampling and manipulation. Seawater was filtered through acid-soaked 200-210 µm mesh to remove mesozooplankton grazers and collected in 20 L acid washed (1 N HCl, rinsed 7-times with MilliQ water) LDPE or PC carboys. Carboys were stored in double-plastic bags and kept in plastic boxes to avoid contact with the ship. All subsequent sampling took place in a custom-made, metal free laminar flow cabinet, dedicated for trace metal clean work using standard clean room procedures.

Experimental setup. Water was homogenised, sampled for dissolved nutrients, flow cytometry, phytoplankton pigments, nucleic acid collection and photo-physiological measurements, with the remainder transferred into pre-treated acid washed (1 N HCl, rinsed 7-times with MilliQ water) 4 L polycarbonate bottles (Nalgene) under laminar flow conditions. Bottles were randomly allocated to five nutrient addition treatments in triplicate: an unamended control, $+NO_3$ (10 µM nitrate final concentration), $+NO_3+FeCl_3$ (10 µM and 1 nM final concentration (ICP-MS 1g/L standard, Fluka), respectively), $+Si(OH)_4$ (10 µM final concentration), nutrient mix ($+NO_3+Si+PO_4+Fe$; 10N : 10Si : 0.625P µM in Redfield proportions and 1 nM Fe respectively). After the addition of nutrients, bottles were capped, gently inverted and lids sealed with parafilm, before being placed into an on-deck, flow-through incubator, exposed to 25 % surface irradiance and in situ temperature conditions.Surface seawater supplying the deck board incubators was 21.94 ± 0.47 during the EAC incubation and 21.57 ± 0.27 during the CCE incubations. This closely matches the *in situ* temperature for both EAC (80 m) and CCE (41 m) communities at the time of sampling (Table 1).

For the EAC experiment, control bottles were sampled daily for maximum quantum yield of photosystem II (F_V/F_M) before being enriched with their respective nutrient or nutrient mix treatment, then re-sealed and returned to the on-deck incubator. The same sampling protocol was used in the CCE; however, no additional nutrient additions were made after the initial amendment to avoid accumulation of excess nutrients. To limit nutrient or microbiological cross-contamination, the same bottles were re-used for identical experimental (nutrient) treatments across the EAC and CCE experiments. Macronutrient analyses were carried out on board by CSIRO Marine and Atmospheric Research (CMAR) according to Cowley et al. (1999). Nutrient measurements had a standard error < 0.7 % and a detection limit of 0.035 µM for NO_x, 0.012 µM for Si and 0.009 µM for PO_4.

After 3 days (72 - 78 h) of incubation, nutrient experiments were terminated. Microbial responses to nutrient additions were quantified by measuring pigments (Chl-a and other accessory pigments), abundance of pico- and nano-phytoplankton and heterotrophic bacteria via flow cytometry, and DNA sequencing for characterising prokaryote and diazotroph community diversity and composition (16S ribosomal RNA, nitrogenase *NifH* subunit targeted, respectively).

Pigment Analysis. Seawater (minimum volume 2.2 L) was filtered under low vacuum (e.g. ≤ 100 mm Hg) onto 25 mm GF/F filters in low light (< 10 µmol photons m^{-2} s^{-1}). Filters were folded in half, blotted dry on absorbent paper, placed into screw-capped cryovials and stored in liquid nitrogen until pigment analysis. In the laboratory, pigments were extracted and analysed using High Performance Liquid Chromatography (HPLC) as described in Hassler et al. (2011). Biomarker pigments were used to infer the distribution of dominant phototrophs. Each biomarker pigment was normalised against chlorophyll-a (the universal pigment in all phytoplankton) to

account for spatial variation in the total phytoplankton biomass. Briefly, biomarkers represent the following phytoplankton groups: Zeaxanthin (Zea) = cyanobacteria; 19'Hexanoyloxyfucoxanthin (19-Hex) = haptophytes; Chlorophyll b (Chl-b) and lutein = Chlorophytes; Alloxanthin (Allo) = cryptophytes, 19'Butanoloxylfucoxanthin (19-But) = pelagophytes; Prasinoxanthin (Prasino) = prasinophytes; Peridinin (Per) = autotrophic dinoflagellates; and Fucoxanthin (Fuco) = diatoms, prymnesiophytes, chrysophytes, pelagophytes and raphidophytes. The photosynthetic (PSC) and photoprotective (PPC) carotenoid pigment contributions were calculated as in Barlow et al. (2007), and the approach of Uitz et al. (2008) was used to assess the taxonomic composition of the phytoplankton community and characterise its size structure. While this method may be subject to error because pigments are shared between different phytoplankton groups, and some groups are spread across different sizes, we apply it in this study to examine relative (not absolute) differences in size structure between water masses and nutrient treatments.

Flow Cytometry. Samples for enumeration of pico- and nano-phytoplankton were fixed with glutaraldehyde (1% v/v final concentration), snap frozen in liquid nitrogen and stored at -80° C. Populations of *Prochlorococcus*, *Synechococcus* and picoeukaryotes were discriminated using side scatter (SSC) and red and orange fluorescence (Marie et al. 1997) using a flow cytometer (LSR II, BD Biosciences). Pigment content per cell was normalised to the fluorescence of standard yellow-green beads (1 μm FluoSpheres®, Life Technologies) that were added to each sample immediately before analysis. Samples for bacterial analysis were stained with SYBR Green I nucleic acid stain (1:10000 final dilution; Molecular Probes) (Marie et al. 1997) and high and low nucleic acid content populations were discriminated according to green fluorescence and side scatter properties (Gasol & Del Giorgio 2000; Seymour, Seuront & Mitchell 2007). Data was analysed using Cell-Quest Pro (BD Biosciences).

DNA extraction and sequence analysis of prokaryote and diazotrophic communities. Water samples (2 L) for DNA analyses were filtered onto 0.2 µm polycarbonate membrane filters (Millipore), snap frozen in liquid nitrogen and stored at -80 °C prior to analysis. Genomic DNA was subsequently extracted using the Power Water DNA extraction kit (MoBio Laboratories, Inc) following the manufacturer's protocols and DNA concentration was quantified using a Qubit® 2.0 fluorometer (Invitrogen). To determine bacterial community composition, the V1-V3 region of the 16S rRNA gene was amplified using the primer sets in Table S1, and sequenced by 454 pyrosequencing (Roche, FLX Titanium; Molecular Research LP) following previously published protocols (Acosta-Martínez et al. 2008; Dowd et al. 2008). 16S rRNA gene sequences were analysed and processed using the Quantitative Insights into Microbial Ecology software (QIIME; Caporaso et al. 2010). Briefly, samples were quality filtered, de-multiplexed and clustered based on 97 % sequence identity using UCLUST (Edgar 2010). Taxonomy was assigned according to the latest version of the SILVA database (111; Quast et al. 2013) and samples were rarefied to the lowest number of sequences to ensure even sampling effort across samples (14,621 sequences per sample).

For N_2-fixing bacteria, the gene encoding a subunit of the enzyme nitrogenase (*NifH*, Zehr, Mellon & Hiorns 1997; Zehr et al. 2003) was amplified and sequenced from genomic DNA using previously published methods (Zehr & McReynolds 1989; Zehr & Turner 2001). A nested PCR protocol was used to amplify an approximately 359 bp region of the *NifH* gene using two sets of degenerate primers listed in Table S1. PCR products were purified using the Ultra Clean PCR Clean-up Kit (MoBio Laboratories, Inc) following the manufacturer's instructions. The *nifH* amplicons were sequenced by 454 pyrosequencing (Roche, FLX Titanium; Molecular Research LP) after an additional 10-cycles PCR with custom barcoded NifH1 and NifH2 primers

under the same reaction conditions (Dowd et al. 2008; Farnelid et al. 2011, 2013). Raw sequences were quality filtered, and de-multiplexed in QIIME (Caporaso et al. 2010). Sequences were clustered at 95 % sequence identity using UCLUST, whereby *nNifH* sequences within 5% identity of a centroid read were assigned as operational taxonomic units (OTUs) (Edgar 2010), then rarefied to 1,050 sequences per sample to ensure even sampling effort, resulting in 989 *NifH* OTUs. Since many of these *NifH* OTUs were singletons, only OTUs with ≥ 100 sequences assigned to them were analysed further (representing 85 % of total *NifH* sequences), resulting in 16 OTUs. Putative taxonomy was assigned using BLASTn (Altschul et al. 1990) against the NCBI Nucleotide collection database, and translated *NifH* sequences were compared to the Ribosomal Database Project's *NifH* protein database using FrameBot (Wang et al. 2013; Fish et al. 2013).

Photophysiological measurements. Photosynthetic efficiency of microbial phototrophs was measured using a Pulse Amplitude Modulated (PAM) fluorometer (Water-PAM; Walz GmbH, Effeltrich, Germany). A 3 ml aliquot of water was transferred to a quartz cuvette and after a 10 min dark-adaptation period, minimum fluorescence (F_O) was recorded. Upon application of a saturating pulse of light (pulse duration = 0.8 s; pulse intensity >3000 µmol photons m^{-2} s^{-1}) maximum fluorescence (F_M) was determined. From these two parameters, F_V/F_M was calculated according to the equation $(F_M - F_O)/F_M$ (Schreiber 2004).

Phytoplankton primary production measurements. Phytoplankton primary production was estimated at the end of the 3-day experiments using small volume ^{14}C incubations as described in Doblin et al. (2011). Carbon uptake rates were normalised to *in situ* chlorophyll *a* concentrations. Carbon fixation-irradiance relationships were then plotted and the equation of Platt, Gallegos & Harrison(1980) used to fit curves to data using least squares non-linear regression.

Photosynthetic parameters included light-saturated photosynthetic rate [P_{max}, mg C (mg Chl-a)$^{-1}$ h^{-1}], initial slope of the light-limited section of the carbon fixation-irradiance curve [α, mg C (mg Chl-a)$^{-1}$ h^{-1} (μmol photons m^{-2} s^{-1})$^{-1}$], and light intensity at which carbon-uptake became maximal (calculated as $P_{max}/ \alpha = E_k$, μmol photons m^{-2} s^{-1}).

Statistical analysis. Differences in microbial composition and diversity between the initial EAC and CCE communities, and between nutrient treatments within each water mass were assessed using analysis of variance (ANOVA; $\alpha = 0.05$). Data were analysed comparing responses at the end of incubation, t_{72} (72 - 78 h), across treatments, as well as comparing the differences over time from the initial water (t_0) to t_{72}. Multiple comparison adjustment of the p-value was made using a Tukey's HSD test. To ensure that the assumption of equal variances for all parametric tests was satisfied, a Levene's test for homogeneity of variance was applied to all data *a priori* and when necessary, data was transformed. All analyses were performed using SPSS statistical software (version 22, IBM, New York USA).

To examine overall changes in microbial assemblages due to nutrient amendment, composition data (i.e. for phototrophs, diagnostic pigments standardised to total Chl-a, flow cytometric counts; for heterotrophs and diazotrophs, rarefied 16S and Nif*H* sequence data, respectively) were square root transformed and a resemblance matrix was generated using Bray-Curtis similarity in the PRIMER software package (Clarke & Warwick 2001). Analysis of similarities (ANOSIM) was used to test the hypothesis that different nutrient amendments would influence microbial composition (Clarke 1993). The contribution of phytoplankton groups to the observed significant differences in community assemblage, as a function of treatment, were determined using Similarity Percentage Analysis (SIMPER; Clarke 1993).

Results

Oceanographic setting. During the voyage, the EAC was flowing southward along the continental shelf edge (Fig. 1B) with a core surface temperature of 23-24 °C. The EAC surface velocity was 1.2 m s^{-1} estimated from altimetry (Fig. 1B, arrows) with the current separating from the coast at ~ 30 °S, forming the Tasman Front. The EAC station (Fig. 1B) had a temperature range of 21.4 to 22.5 °C and a salinity of 35.45 to 35.52 in the upper 200 m of the water-column. The cyclonic eddy, south of the EAC station, was sampled on 25th October 2015 when it centred at 32 °S adjacent to the continental shelf. The CCE had a temperature range of 14.3 to 21.8 °C and a salinity of 35.26 to 35.54 in the upper 200 m of the water-column.

Dissolved macronutrient stocks indicated the potential for widespread N limitation in the EAC and adjacent shelf and Tasman Sea (offshore) waters (Fig. 2A), with nitrate deficit ($N^* = [NO_3^-] - 16[PO_4^{3-}]$) occurring to at least 200 m (overall mean for all depths ± SD = -1.9 ± 0.53 µM; Fig. 2B). Oxidised N (nitrate) was detectable at the Chl-a fluorescence maximum in the EAC (80 m) and CCE (41 m), ranging between 0.1 and 0.3 µM (Fig. 3), with dissolved phosphate being ~0.1 µM in both water masses (Table 1).

Microbial community composition and diversity in different water masses. Initial Chl-a concentrations were relatively low (0.106 and 0.336 µg L^{-1}), but distinct (p-value < 0.05), in the EAC and CCE, respectively (Table 1; t0 Fig. 4A and B). The most abundant phototroph in the EAC was the cyanobacterium *Prochlorococcus*, whereas in the CCE it was *Synechocccus* (Fig. S1). A significant proportion of larger phototrophs in the EAC contained 19'-hexanoyloxyfucoxanthin (Hex-Fuco; t0 Fig 4E), exclusively found in haptophytes, including the coccolithophores (Liu et al. 2009). However, in the CCE, fucoxanthin (found in Phaeophyta and most other heterokonts), was the dominant accessory pigment, largely indicative of diatoms (t0

Fig. 4D). Pigment ratios suggested the size structure of the EAC phototrophic community was dominated by pico- and nano-plankton (< 2 µm) and in the CCE by microplankton (≥ 20 µm; t0 Fig. 5A and B, respectively). Pigment richness was 30% higher in the CCE than in the EAC, and phototrophic alpha-diversity was ~40% higher (Shannon's index calculated using HPLC pigment data = 1.02 ± 0.05 compared to 0.64 ± 0.02 in the EAC; average ± SD here and throughout).

With respect to the heterotrophs, the total abundance of bacteria was similar in both water masses (~8.5 x 10^5 cells ml^{-1}; t0 Fig. 5I and J) but there was a greater proportion of high DNA bacteria in the CCE (47 ± 4 vs 39 ± 2 % in the EAC). The greatest proportion of bacterial 16S rRNA sequences in both water masses belonged to the alpha-proteobacteria (SAR11 and SAR116 clade), Rhodobacteriaceae, as well as *Synechococcus* and *Prochlorococcus* (Fig. 6) but there was no difference in bacterial alpha-diversity between water masses (Shannon's index in EAC = 3.20 ± 0.13 compared to 3.10 ± 0.19 in the CCE). Heterotrophic *NifH* gene sequences were detected in the EAC and were primarily attributable to members of the gamma-, beta-, and delta-proteobacteria. Initial CCE samples were not available (cryovials broken in storage); however control CCE treatments contained phototrophic and heterotrophic diazotrophs, including *Trichodesmium*, UCYN-A and gamma-proteobacterial *NifH* sequences.

Nutrient-induced shifts in the phototrophic community. After 3 days, there was a large positive effect of NFe and the nutrient Mix (N,P,Si,Fe) on the total Chl-a concentration in the EAC community (Fig. 4A), which occurred alongside an increase in fucoxanthin relative to Chl a in the NFe and Mix treatments (p-value ≤ 0.026; Fig. 4C), suggesting a greater relative abundance of diatoms (Table 2). The relative abundance of haptophytes (as indicated by pigment Hex-Fuco) showed a declining trend across all treatments, but by the end of the experiment haptophytes were least abundant in the NFe treatment (p-value ≤ 0.031; Fig. 4E).

Prochlorococcus (as determined by flow cytometric counts) decreased in all treatments including the controls (Fig. 5G), but *Synechococcus* abundance declined only in the Mix treatment (Fig. 5E). Collectively, there was a decrease in picoeukaryote abundance in all but the NFe EAC bottles by day 3 (p-value < 0.05; Table 2), with the phototrophic community overall showing a significant cell size increase into the micro size class (nominally ≥ 20 µm) with N amendment (p-value < 0.05; Fig. 5A), as estimated through pigment ratios (Uitz et al. 2008). Taken as a whole, the largest shift in phototrophic community composition and structure was in the mix treatment relative to all other treatments (SIMPER, >75% dissimilarity), which was attributed mainly to the decrease in picoeukaryotes. Importantly, the EAC community was more similar to the t_0 CCE community after nutrient amendment, particularly with NFe addition (Global R = 0.48, p-value < 0.05; Fig 7C).

In contrast, within the CCE, addition of N, NFe and Mix caused a significant increase in Chl-a relative to the initial community (Fig. 4B; Table 2). Consistent with the patterns seen in the EAC, Fucoxanthin:Chl-a increased in NFe and Mix bottles (and in the N treatment), which was concomitant with a decline in haptophytes (Hexo-Fuco:Chl-a; Fig. 4D and F; Table 2). There was a decrease in picoeukaryotes in the Mix treatment relative to unamended controls (Fig. 5D), as well as a measurable increase in *Prochlorococcus* with NFe amendment (Fig. 5H). *Synechococcus* showed little effect of nutrient amendment in the CCE but declined when all nutrients were added together (p-value < 0.05; Fig. 5F; Table 2). Similar to the EAC, there was an overall increase in cell size of the CCE phototrophic assemblage into the micro size class with NFe and Mix amendment (p-value < 0.05; Fig. 5B). The Mix addition caused the greatest shift in cell size structure, decreasing the abundance of small cells by an order of magnitude (Fig. 5). Similar to the EAC community, the largest shift in phototrophic community composition and

structure was in the Mix relative to all other treatments (SIMPER, ≥55% dissimilarity), mainly due to the decrease in *Synechococcus* and picoeukaryotes.

Nutrient-induced shifts in the heterotrophic community. Nutrient-induced changes in the EAC bacterioplankton community were also detected by the end of the experiment (Figs. 5I, 6, 7). There was a significant (but relatively small) decrease in the relative abundance of sequences matching SAR11 Surface 1 and SAR116 clades, and an increase in relative abundance of *Synechococcus* with N, NFe, Mix addition, with the greatest dissimilarity in bacterial community composition observed between the t_0 and NFe treatments (SIMPER, 29 % dissimilarity). These shifts in SAR11, SAR116 and *Synechococcus* relative abundance contributed to 3, 2 and 2 % dissimilarity between the t_0 and NFe treatments respectively (Fig.6; SIMPER). This pattern of increasing *Synechococcus* sequence abundance was consistent with the patterns of *Synechococcus* abundance revealed from flow cytometry (Fig. 5E). Within EAC nutrient addition treatments, the greatest dissimilarity was observed between bacterioplankton communities in the NFe and Si amendments (SIMPER, 29 % dissimilarity). A relative decrease in *Synechococcus* with Si, and an increase in the SAR116 clade and *Prochlorococcus*, contributed 3, 2 and 2 % to the dissimilarity between NFe and Si treatments, respectively (Fig. 6; SIMPER).

In the CCE bacterioplankton composition was distinct from the EAC in unamended controls after 3 days (ANOSIM, Global R: 1.00, p-value < 0.01; Fig. 7F), with the SAR116 clade and Rhodobacteraceae more abundant in the CCE than in the EAC, and SAR11 surface clade and *Prochlorococcus* less abundant (Fig. 6. Total heterotrophic bacterial abundance in the CCE doubled after 3 days with Si and Mix addition, unlike the EAC community (Fig. 5I and J).

However, there was no appreciable shift in bacterioplankton diversity between nutrient addition treatments (Fig. 7E; ANOSIM, Global R: 0.14, p-value > 0.05).

Similar to the patterns observed in the overall bacterioplankton compositon, diazotroph diversity in the EAC shifted following nutrient amendment (ANOSIM, Global R: 0.79, p-value = 0.001; Fig. 7G). Nutrient addition shifted the composition of diazotrophs from gamma-, beta-, and delta-proteobacteria toward several Cluster 1 gamma-proteobacterial *NifH* sequences (*NifH* OTU 608, 2012 and 95), sharing ≥ 89 % amino acid identity with *Pseudomonas stutzeri* (Moisander et al. 2014, 2012), which comprised negligible proportions of initial EAC *NifH* sequences. Shifts in the relative abundance of the three different gamma-proteobacterial *NifH* OTUs contributed to a substantial proportion of the dissimilarity between diazotroph communities detected in EAC nutrient treatments. For example, *NifH* OTU608 dominated NFe bottles, comprising up to 97 % of *NifH* sequences and was responsible for 33 % of the average dissimilarity between t_0 and NFe (SIMPER, 83 % total dissimilarity). In Si bottles, *NifH* OTU2012 represented up to 87 % of *NifH* sequences detected, and contributed 41 % to the average dissimilarity between the t_0 and Si bottles (SIMPER, 65 % dissimilarity). Similarly *NifH* OTU95 comprised up to 89 % of *NifH* sequences in the Mix treatment and was responsible for 22% of the dissimilarity between the t_0 and diazotrophs in the Mix addition.

In contrast to *NifH* sequences retrieved from EAC nutrient treatments, the dominant *NifH* OTU across CCE nutrient amendments was OTU2331, which shared 90 % amino acid identity to the genus *Coraliomargarita* of the Verrucomicrobia. In addition, sequences sharing 95 % *NifH* amino acid identity with *Trichodemsium erythraeum* (OTU181) and *Candidatus Atelocyanobacterium thalassa* (UCYN-A; OTU1321 and OTU50), were detected in the unamended CCE diazotroph assemblages, but no such cyanobacterial *NifH* sequences were

present in the EAC. Differences in the relative abundance of these cyanobacterial diazotrophs were observed between treatments, such as an increase in OTU181 from a maximum of 15 % in the control to 62 % in the Si treatment, there were also significant shifts in diazotroph composition between nutrient addition treatments (Fig. 7H) (ANOSIM, Global R: 0.69, p-value = 0.004). Notably, there were no *NifH* sequences detected in the CCE Mix treatment.

Time-dependent response to nutrient amendment: subcellular to community-level. Daily sampling of incubation bottles following nutrient amendment captured a cascade of effects at the cellular, population and community level, indicating differences in the speed of response by different microbes to nutrient resupply. Despite lower phytoplankton biomass, the EAC community took up ~10 times more nitrate than the CCE community within the first 24 h (Fig. 8A and B). , Net nitrate uptake in the EAC (averaged over day 1 to 3) was greatest in the Mix (2.98 ± 0.88 μM d^{-1}), and NFe and N treatments (~2 μM d^{-1}), but was < 0.3 μM d^{-1} in all other treatments. In the CCE, the level of nitrate uptake was an order of magnitude lower, with rates ranging from 0.02 to 0.25 μM d^{-1} (in the control and Mix, respectively). Net phosphate uptake by both communities was relatively constant across nutrient amendments (~0.1 and ~0.01 μM d^{-1} in the EAC and CCE, respectively), with the exception of 30% higher rates in the EAC Mix treatment (Fig. S3). Net silicate uptake rates in the EAC were greater than the CCE (~0.1 vs ~0.05 μM d^{-1}, respectively), with rates increasing significantly (≥ 6 times) when Si was added alone or with N, P and Fe (i.e., Mix treatment; Fig. S3). Total dissolved iron (TDFe) concentrations at the end of the experiment were 0.38 ± 0.07 nM in the unamended EAC control bottles, and 1.32 ± 0.23 nM in the CCE controls (Fig. S3), suggesting a strong Fe consumption and thus a limited Fe potential contamination in the experiment (spikes were 10 nM).

To illustrate the impact of nutrient amendment at the cellular, population and community level in the EAC and CCE, Fig. 8 shows time-dependent responses to the N treatment. The cellular pigment content (as estimated using flow cytometer fluorescence emission detected at red/orange wavelengths, corresponding to Chl-a/phycoerythrin) of EAC phototrophs in the N treatment was relatively constant over the first 48 h, but then increased in both phycoerythrin-containing prokaryotes and Chl-a-containing cells by t_{72} (Fig. 7C; Tables 2 and 3). In the CCE, N addition caused rapid synthesis of Chl-a (but not phycoerythrin) in the first 24 h. By day 3 however, phycoerythrin-containing prokaryotes in the CCE had doubled their pigment content, in a manner that was similar to the observations in the EAC (Fig. 7D).

The initial ranked order abundance of microbial populations (as determined flow cytometrically) was different in the EAC and CCE and showed variable temporal dynamics. N amendment of the EAC community resulted in a doubling of total bacteria abundance within the first 24 h (Fig. 8E), but they then decreased to initial concentrations by t_{72}. The abundance of all but the large picoeukaryote population declined in the EAC under N amendment, resulting in overall negative phototrophic growth over the three day experiment (-0.153 ± 0.016 d^{-1}; Table S2). In contrast, the abundance of all CCE phototroph populations increased within the first 24 h following N amendment (Fig. 8D), and yielded significant positive growth during the experiment (0.262 ± 0.043 d^{-1}).

Nutrient amendment caused a minor decline in the maximum quantum yield of PSII (F_V/F_M) in the EAC microbial community with N addition (p-value = 0.013; Table 2), but had no effect on F_V/F_M in the CCE community, remaining > 0.65 in the unamended controls (Fig. 8A). The light saturating irradiance I_K was ~50% lower in the EAC, reflecting the greater depth of the sampled community (Table 1), and despite lower phytoplankton biomass, carbon fixation rates in

447 unamended EAC bottles were higher than that of CCE controls (Fig. 8G and H). N amendment
448 of the EAC community lead to a significant increase in light utilisation efficiency (α) and light
449 saturated photosynthetic rate (P_{max}) with no change in minimum saturating irradiance (I_K)
450 between the control and N enriched cells. There was however, a significant decline in I_K in the
451 NFe treatment (p-value < 0.05Table 2). In the CCE, there was a significant increase in α and P_{max}
452 with both N and NFe addition, with I_K lowest in the NFe treatment. There was a 1.7 times
453 increase in the maximum rate of primary productivity in the N amended treatment for the EAC
454 (p-value <0.001), compared with a 2.7 times increase in the CCE (p-values < 0.001; Fig. 8G and
455 H). Co-addition of NFe resulted in a decrease in PP in the EAC (0.4 fold change), but a 6.28 fold
456 increase in PP in the CCE. This suggests stronger limitation of primary productivity in the CCE,
457 with a greater proportional increase in P_{max} with NFe compared to N addition.

458

459 **Discussion**

460 The intensification of western boundary currents in the global ocean (Wu et al. 2012) raises
461 significant questions about their impact on microbial composition and biogeochemical activity,
462 particularly in light of the potential for WBCs to promote meso-scale eddy formation (Mata et al.
463 2007) and induce nutrient upwelling (Roughan & Middleton 2002). Here we show clear
464 differences in the vertical nutrient structure of a cyclonic cold-core eddy relative to adjacent
465 waters, and an increase in microbial diversity and size structure of an eddy assemblage relative to
466 an adjacent western boundary current, the EAC. Our results indicate that cyclonic eddies
467 increase delivery of N to the upper ocean but also increase the biological demand for Fe that is

necessary to sustain the growth of large-celled phototrophs and potentially support the diversity of diazotrophs over longer time-scales.

Responses of microbes to nutrient amendment.

Previous studies in the Tasman Sea region have determined that surface phytoplankton communities are limited by N (Hassler et al. 2011; Hassler et al. 2014; Ellwood et al. 2013), and that diazotrophs (cyanobacteria that are able to bypass nitrate limitation by fixing atmospheric N) inhabit waters to ~100 m following nutrient draw-down over the summer (Moisander et al. 2010). Our observations show that EAC phytoplankton sampled at 80 m below the surface are also N limited, and that upwards displacement of isopycnal surfaces induced by a cyclonic eddy introduces nutrients into the euphotic zone to alleviate potential N limitation (Fig. 4). Phytoplankton in the CCE (sampled at ~40 m) were also limited by N, but rates of carbon fixation more than doubled under NFe relative to N amendment, likely due to the different species composition underpinning primary productivity. In both water masses, a positive response in Chl-a was also seen with addition of N+Fe+Si+P, suggesting co-limitation by multiple nutrients in both water masses, likely a result of different nutrient requirements by different phototrophs. Uplift of N together with Fe and other nutrients would therefore increase the rate of biomass production in the eddy as well as increase the relative abundance of diatoms, both of which could act to increase export production relative to adjacent waters.

While the starting communities in the EAC and CCE were distinct, microbial phototrophs showed similar responses to nutrient amendment in both water masses, with NFe addition to the EAC resulting in phototrophs more similar to those in the initial CCE community (Fig. 7C). Fucoxanthin containing cells (likely diatoms that contribute significantly to export production;

Honjo et al. 1995) became more prevalent in NFe and Mix treatments, whereas haptophytes clearly diminished under these amendments. Similarly, peridinin-containing dinoflagellates were initially present in both communities, but their abundance declined with nutrient amendment, becoming undetectable amongst other EAC microbes at the end of our experiment. *Prochlorococcus* was an order of magnitude more abundant in the EAC relative to the CCE, consistent with the warmer "tropical" signature of this western boundary current (Seymour et al. 2012), and declined in abundance in the Mix treatment. In the CCE samples, *Prochlorococcus* similarly decreased in the Si and Mix treatments. *Synechococcus* had a positive response to bottle enclosure but unlike other studies (Moisander et al. 2012), we found that its abundance was similar in control and enriched treatments. Maximum net growth rates were observed in the eddy NFe bottles for *Prochlorococcus* (0.345 ± 0.047 d^{-1}), small picoeukaryotes (0.212 ± 0.033 d^{-1}) and large picoeukaryotes (i.e., nano-eukaryotes; 0.297 ± 0.059 d^{-1}), but for *Synechococcus*, maximum growth was found in CCE controls (0.324 ± 0.047 d^{-1}, relative to 0.194 ± 0.035 d^{-1} with NFe amendment).

Among the heterotrophic bacteria, initial EAC and CCE populations displayed similar abundance and alpha-diversity, and nutrient amendment lead to compositional shifts in both water masses. Addition of nitrate to the EAC community caused a doubling of total bacteria abundance within the first 24 h. Bacteria also became more abundant in the CCE community after 3 days within the Si and Mix bottles. Elevated bacteria abundance is likely to have arisen through increased dissolved organic matter (DOM) production by the resident community via several potential mechanisms: (1) mortality and cell lysis; (2) elevated rates of DOM release due to nutrient supplementation; and (3) altered microbial composition. While we did not measure rates of

512 DOM production, our data certainly demonstrate coupling between autotrophs and heterotrophs,
513 just as in a previous study (Baltar et al. 2010).

514 **Diazotroph relative abundance and diversity.** Across the global ocean, the main supply of
515 nitrogen into surface waters is via transport from below the thermocline, but in many regions
516 significant amounts of new nitrogen may also be supplied via nitrogen fixation (Capone et al.
517 2005; La Roche & Breitbarth 2005). Our molecular analyses revealed the presence of
518 heterotrophic gamma-proteobacterial diazotrophs in the sub-surface EAC microbial community,
519 whereas cyanobacterial diazotrophs (i.e., *Trichodesmium* and UCYN-A) were detected in the
520 CCE. Given the relatively high iron requirement of diazotrophs (Kustka et al., 2003), as well as
521 their low reliance on dissolved inorganic N, we expected to see a divergent response of the
522 diazotrophs to nutrient amendment. Indeed, in the Mix bottles, diazotrophs became undetectable
523 in the CCE samples, and were clearly outcompeted by the eukaryote phototrophs. Nutrient
524 addition resulted in *NifH* OTU2331 becoming more prominent across CCE nutrient amendments.
525 This OTU shares 90 % amino acid identity to the genus *Coraliomargarita* of the
526 Verrucomicrobia, and was not present amongst the EAC diazotrophs. In the EAC, nutrient
527 addition caused a shift from the mixed proteobacterial community observed at t0, to *NifH*
528 OTU608, *NifH* OTU2012 and *NifH* OTU95. These OTUs represent distinct taxa at the 95%
529 sequence similarity level, yet share the same % identity at the amino acid level, falling within the
530 same clade of Cluster 1 gamma-proteobacterial diazotrophs. The physiology or genome content
531 of these taxa remains completely unknown, but they seem to be abundant in warm, oligotrophic
532 surface waters globally (Langlois et al., 2005). In the southwestern Pacific, the abundance of this
533 group has been shown to be correlated to DOC concentration, and to increase with Fe and P
534 addition (Moisander et al., 2012). In contrast, the dominant diazotroph in the CCE was an OTU

sharing 95 % *NifH* amino acid identity with *Trichodemsium erythraeum* (OTU181) and OTUs matching *Candidatus Atelocyanobacterium thalassa* (UCYN-A; OTU1321 and OTU50). UCYN-A is the dominant diazotroph in the Coral Sea (source of the EAC) during the austral spring (Messer et al., 2015), and is also relatively abundant in the western South Pacific (Moisander et al., 2010). UCYN-A abundance has previously been shown to increase in response to Fe and organic carbon additions (Moisander et al., 2012), while Fe has also been shown to increase the rate of N_2 fixation by UCYN-A (Krupke et al., 2015).

Our observations demonstrate the presence of heterotrophic N_2-fixing organisms in sub-surface waters with strong nitrate deficiency (but not necessarily low nitrate concentration; Fig. 2); however, a remaining research need is to conduct N_2-fixation rate measurements in conjunction with diazotroph diversity assessment to verify whether this process represents a significant source of new N within and outside eddies, and whether changes in N_2-fixation are due to a shift in diversity or a change in *NifH* expression.

Physiological responses to nutrient supply. At the cellular level, N addition caused rapid pigment synthesis (doubling of normalised fluorescence per cell) in the CCE assemblage within the first 24 h after amendment, indicating that nutrient uplift could initially cause 'greening' in the absence of an increase in cellular biomass (Behrenfeld et al. 2015). By the end of our experiments, both phycoerythrin and Chl-a quotas increased in both water masses with N amendment, concomitant with an increase in total Chl-a, suggesting both pigment synthesis and biomass production contributed to elevated Chl-a. These observations are of obvious importance for the accurate interpretation of satellite and other in situ Chl-a fluorescence data within meso-scale eddy features.

557 Photophysiological changes such as a decline in PSII turnover time, cross-sectional area and
558 increased electron transport rates have been detected upon relief of nutrient limitation (Milligan,
559 Aparicio & Behrenfeld 2012). We detected minimal change in the photochemical efficiency
560 (maximum quantum yield of PSII) with nutrient amendment, but there were measureable
561 changes in the shape of the photosynthesis-irradiance (P-I) curve. Nitrate amendment of the EAC
562 community increased light utilisation efficiency and light saturated photosynthetic rates,
563 indicating increased photosynthetic electron transport and antenna size. Our flow cytometry data
564 suggest that this was likely due to increased chlorophyll quota rather than an increase in cross
565 sectional area (Fig. 7D). In the CCE community, the greatest change in carbon fixation (P-I)
566 parameters was measured in the NFe treatment, suggesting an increase in PSII units per cell
567 (detected via increased pigment quotas after 24 h), as well as an increase in total photosynthetic
568 biomass, resulting in increased electron transport rates and light capturing capacity.

569 **Nutrient uptake dynamics.** Initial uptake rates of nitrate (i.e. within the first day) by the EAC
570 community were 10 times higher than in the CCE despite 3-fold lower phytoplankton biomass.
571 This is consistent with the opportunistic nutrient uptake strategies of phytoplankton in
572 oligotrophic habitats (McCarthy & Goldman 1979) and the theory that fast growing algae (with
573 small cell size) are stimulated by short-term nutrient supply (Pederson & Borum 1996).
574 However, it is unlikely that such high nutrient uptake rates would be sustained in the EAC,
575 largely because nutrient inputs (of the magnitude used in our experiments) are episodic and often
576 coincide with major physical disturbances such as cyclones (e.g. Law et al. 2011). A comparison
577 of the initial EAC and CCE communities suggests that prolonged nutrient inputs within cyclonic
578 eddies results in a shift toward larger cells which generally have greater capacity for nutrient
579 storage and higher nutrient requirements for growth (Litchman et al. 2007).

Despite these potential experimental artefacts, the relative differences in nutrient demand between treatments show that maximum net uptake rates in both water masses occurred when all macronutrients were added together, compared to treatments which contained a surplus of N, P or Si relative to other macronutrients and iron. Under N amendment, uptake ratios of N:P in the EAC were ~20 compared to ~10 in the CCE, and uptake ratios of N:Si were ~10 and 4 in the EAC and CCE, respectively, but they were closer to Redfield (Si:N:Pi = 1:1:16) in the Mix treatment (Fig. S2). This indicates that the vertical distribution of nutrients relative to one another will regulate microbial responses to eddy-induced uplift, as has been shown by Bibby and Moore (2011) with respect to N:Si in the sub-tropical north Atlantic and central Pacific near Hawai'i.

Conclusions

Phytoplankton community structure plays an important role in the ecology and biogeochemistry of pelagic ecosystems including the export of organic matter to the deep ocean and the sequestration of carbon (Follows & Dutkiewicz 2011; Karl et al. 2012). Here we show that cyclonic eddies enhance primary production in this WBC region by delivering nitrate to the upper ocean. The enhanced productivity was driven largely by an increase in the abundance of diatoms, with a concomitant decline in the abundance of haptophytes and peridinin-containing dinoflagellates.

This study confirms the low-nutrient low Chl-a status of the Eastern Australian Current (EAC) to sub-surface depths of ~80 m, and provides the first evidence of N and Fe co-limitation in an adjacent cyclonic eddy, demonstrating that such meso-scale features have the potential to increase internal nutrient inputs into the upper ocean and thereby change microbial composition

and nutrient demand. Importantly, eddies may provide a critical compensatory mechanism to enrich the upper ocean and counteract increasing stratification occurring under climate change (Matear et al. 2013). The divergent response of large phototrophs and diazotrophs in our nutrient amendment experiments suggests that N_2-fixing cyanobacteria and heterotrophic bacteria are an important functional group to include in biogeochemical models, whose abundance and diversity have been under-appreciated in this region until recently (Messer et al., 2015).

Acknowledgements.

We thank the officers and crew of the *R/V Southern Surveyor* and the Bio-optics voyage participants, particularly Massimo Pernice (Instituto de Ciencias del Mar- Consejo Superior de Investigacion Cientifica, Spain) for assistance with sampling, Andrew Bowie for dissolved Fe flow injection analyses, as well as Jennifer Clark (University of Technology Sydney) for flow cytometry analyses.

References

Acosta Martinez V, Dowd SE, Sun Y, Allen V (2008) Tag-encoded pyrosequencing analysis of bacterial diversity in a single soil type as affected by management and land use. Soil Biology and Biochemistry. 40(11):2762-2770.

Altschul S, Gish W, Miller W, Myers E, Lipman D (1990) Basic local alignment search tool. Journal of Molecular Biology **215**:403–410. http://www.sciencedirect.com/science/article/pii/S0022283605803602 (Accessed December 13, 2013).

Baltar F, Arı´stegui J, Gasol JM, Lekunberri I, Herndl GJ (2010) Mesoscale eddies: hotspots of prokaryotic activity and differential community structure in the ocean. The ISME Journal **4**: 975–988.

Barlow RG, Stuart V, Lutz V, Sessions H, Sathyendranath S, Platt T, Kyewalyanga M, Clementson L, Fukasawa M, Watanage S, Devred E (2007) Seasonal pigment patterns of surface phytoplankton in the subtropical southern hemisphere. Deep-Sea Research I **54**:1687-1703.

Behrenfeld M (2011) Biology: Uncertain future for ocean algae. Nature Climate Change **1**:33–34 doi:10.1038/nclimate1069.

633 Behrenfeld MJ, O'Malley RT, Boss ES, Westberry TK, Graff JR, Halsey KH, Milligan AJ,
634 Siegel DA and Brown TB (2015) Revaluating ocen warming impacts on global phytoplankton.
635 Nature Climate Change doi: 10.1038/NCLIMATE2838.

636 Bibby TS, Gorbunov MY, Wyman KW, Falkowski PG (2008) Photosynthetic community
637 responses to upwelling in mesoscale eddies in the subtropical North Atlantic and Pacific Oceans.
638 Deep-Sea Research II **55**: 1310-1320.

639 Bibby TS, Moore CM (2011) Silicate:nitrate ratios of upwelled waters control the phytoplankton
640 community sustained by mesoscale eddies in sub-tropical North Atlantic and Pacific.
641 Biogeosciences **8**: 657–666.

642 Brzezinski MA, Nelson DM (1989). Seasonal changes in the silicon cycle within a Gulf Stream
643 warm-core ring. Deep-Sea Research 36: 1009-1023.

644 Capone DG, Burns JA, Montoya JP, Subramaniam A, Mahaffey C, Gunderson T, Michaels AF,
645 Carpenter EJ. (2005) Nitrogen fixation by *Trichodesmium* spp.: An important source of new
646 nitrogen to the tropical and subtropical North Atlantic Ocean. Global Biogeochemical Cycles
647 19(2) GB2024

648 Caporaso J, Kuczynski J, Stombaugh J, Bittinger K, Bushman F, Costello EK, et al. (2010).
649 QIIME allows analysis of high-throughput community sequencing data. Nature Methods **7**:335–
650 336. http://dx.doi.org/10.1038/nmeth0510-335 (Accessed December 7, 2013).

651 Chelton DB, Schlax MG, Samelson RM (2011) Global observations of nonlinear mesoscale
652 eddies. Progress in Oceanography **91**:167–216.

653 Clarke K (1993). Non-parametric multivariate analyses of changes in community structure.
654 Australian Journal of Ecology **18**:117–143. http://onlinelibrary.wiley.com/doi/10.1111/j.1442-
655 9993.1993.tb00438.x/full (Accessed January 13, 2014).

656 Clarke K, Warwick R (2001) Change in marine communities: an approach to statistical analysis
657 and interpretation 2nd Edition. PRIMER-E Ltd: Plymouth
658 http://www.opengrey.eu/item/display/10068/595716 (Accessed January 14, 2014).

659 Cowley R, Critchley G, Eriksen R, Latham V, Plaschke R, Rayner M, Terhell D (1999) CSIRO
660 Marine Laboratories Report 236 Hydrochemistry Operations Manual. Technical report, CSIRO
661 Marine Laboratories, Hobart, Australia.

662 Deutsch C, Weber T (2012) Nutrient Ratios as a Tracer and Driver of Ocean Biogeochemistry
663 Annual Review of Marine Science **4**:113–41.

664 Doblin MA, Ralph PJ, Petrou KL, Shelly K, Westwood K, van den Enden R, Wright S, Griffiths
665 B (2011) Diel variation of chl-a fluorescence, phytoplankton pigments and productivity in the
666 Sub-Antarctic Zone. Deep Sea Research II: Topical studies in oceanography **58**:2189-2199.

667 Dowd SE, Callaway TR, Wolcott RD, Sun Y, McKeehan T, Hagevoort RG, et al. (2008)
668 Evaluation of the bacterial diversity in the feces of cattle using 16S rDNA bacterial tag-encoded

669 FLX amplicon pyrosequencing (bTEFAP). BMC Microbiology **8**:125.
670 http://www.pubmedcentral.nih.gov/articlerender.fcgi?artid=2515157&tool=pmcentrez&renderty
671 pe=abstract (Accessed January 23, 2014).

672 Edgar RC (2010) Search and clustering orders of magnitude faster than BLAST. Bioinformatics
673 **26**:2460–2461. http://www.ncbi.nlm.nih.gov/pubmed/20709691 (Accessed November 7, 2013).

674 Ellwood MJ, Law CS, Hall, J., Boyd PW (2013) Relationships between nutrient stocks and
675 inventories and phytoplankton physiological status along an oligotrophioc meridional transect in
676 the Tasman Sea. Deep-Sea Research I **72**:102-120.

677 Everett JD, Baird ME, Oke PR, Suthers IM (2012) An Avenue of Eddies: Quantifying the
678 biophysical properties of mesoscale eddies in the Tasman Sea. Geophysical Research Letters **39**:
679 L16608 doi:10.1029/2012GL053091.

680 Everett JD, Baird ME, Roughan M, Suthers IM, Doblin MA (2014) Relative impact of seasonal
681 and oceanographic drivers of surface chlorophyll-a along a western boundary current. Progress
682 in Oceanography **120**:340-351.

683 Farnelid H, Andersson AF, Bertilsson S, Al-Soud WA, Hansen LH, Sørensen S, et al. (2011)
684 Nitrogenase gene amplicons from global marine surface waters are dominated by genes of non-
685 cyanobacteria. PLoS One **6**:e19223.
686 http://www.pubmedcentral.nih.gov/articlerender.fcgi?artid=3084785&tool=pmcentrez&renderty
687 pe=abstract (Accessed March 14, 2013).

688 Farnelid H, Bentzon-Tilia M, Andersson AF, Bertilsson S, Jost G, Labrenz M, et al. (2013).
689 Active nitrogen-fixing heterotrophic bacteria at and below the chemocline of the central Baltic
690 Sea. The ISME Journal **7**:1413–1423.

691 Fish JA, Chai B, Wang Q, Sun Y, Brown CT, Tiedje JM, et al. (2013) FunGene: the functional
692 gene pipeline and repository. Frontiers of Microbiology **4**:291.
693 http://www.pubmedcentral.nih.gov/articlerender.fcgi?artid=3787254&tool=pmcentrez&renderty
694 pe=abstract (Accessed February 5, 2014).

695 Foldager Pedersen M, Borum J (1996) Nutrient control of algal growth in estuarine waters.
696 Nutrient limitation and the importance of nitrogen requirements and nitrogen storage among
697 phytoplankton and species of macroalgae. Marine Ecology Progress Series **142**:261-272.

698 Follows MJ, Dutkiewicz S, Grant S, Chisholm SW (2007) Emergent biogeography of microbial
699 communities in a model ocean. Science **315**:1843–1846.

700 Follows MJ, Dutkiewicz S (2011) Modeling Diverse Communities of Marine Microbes. Annual
701 Review of Marine Science **3**:427–451.

702 Gasol JM, Del Giorgio PA (2000) Using flow cytometry for counting natural planktonic bacteria
703 and understanding the structure of planktonic bacterial communities. Scientifica Marina **64**:
704 197−224

Gaube P, McGillicuddy DJ Jr, Chelton DB, Behrenfeld MJ, Strutton PG (2014) Regional variations in the influence of mesoscale eddies on near-surface chlorophyll. Journal of Geophysical Research Oceans **119**:8195–8220.

Hagino K, Onuma R, Kawachi M, Horiguchi T (2013) Discovery of an Endosymbiotic Nitrogen-Fixing Cyanobacterium UCYN-A in *Braarudosphaera bigelowii* (Prymnesiophyceae). PLoS ONE **8**: e81749. doi:10.1371/journal.pone.0081749

Hassler C, Djajadikarta RJ, Doblin MA, Everett JD, Thompson P (2011) Characterisation of water masses and nutrient limitation of phytoplankton in the separation zone of the East Australian Current in spring 2008. Deep Sea Research II, special issue on East Australian Current. **58**:664-677.

Hassler CS, Ridgway K, Bowie AR, Butler ECV, Clementson L, Doblin MA, Ralph P, Law CS, Davies DM, van der Merwe P, Watson R, Ellwood, MJ (2014) Primary productivity induced by Iron and Nitrogen in the Tasman Sea-An overview of the PINTS expedition. Marine and Freshwater Research **65**:517-537.

Honjo S, Dymond J, Collier R, Manganini SJ (1995) Export production of particles to the interior of the equatorial Pacific Ocean during the 1992 EqPac experiment. Deep Sea Research II **42**:831-870.

Hood RR, Laws EA, Armstrong RA, Bates NR, Brown CW, Carlson CA, Chai F, Doney SC, Falkowski PG, Feely RA, Friedrichs MAM, Landry MR, Moore KJ, Nelson DM, Richardson TL, Salihoglu B, Schartau M, Toole DA, Wiggert JD (2006) Pelagic functional group modeling: Progress, challenges and prospects. Deep-Sea Research Part II-Topical Studies in Oceanography **53**:459-512.

Karl DM, Church MJ, Doreb JE, Letelier RM and Mahaffey C (2012) Predictable and efficient carbon sequestration in the North Pacific Ocean supported by symbiotic nitrogen fixation. Procedings National Academy Science **109**:1842–1849.

Kustka AS, Sañudo-Wilhelmy S, Carpenter EJ, Capone DG, Raven, JA (2003) A revised estimate of the iron efficiency of nitrogen fixation with special reference to the marine cyanobacterium *Trichodesmium* spp. (cyanophyta). Journal of Phycology **39**:12–25.

Krupke A, Mohr W, LaRoche J, Fuchs BM, Amann RI, Kuypers MM (2015) The effect of nutrients on carbon and nitrogen fixation by the UCYN-A-haptophyte symbiosis. ISME J. **9**:1635-47.La Roche J, Breitbarth E (2005) Importance of diazotrophs as a source of new nitrogen in the ocean. Journal of Sea Research **53**:67-69.

Langlois RJ, LaRoche J, Raab PA (2005) Diazotrophic Diversity and Distribution in the Tropical and Subtropical Atlantic Ocean. Applied and Environmental Microbiology 71:7910–7919.

Law CS, Woodward EMS, Ellwood MJ, Marriner A, Bury SJ, Safi KA (2011) Response of surface nutrient inventories and nitrogen fixation to a tropical cyclone in the southwest Pacific. Limnology and Oceanography **56**:1372–1385.

Liu H, Probert I, Uitz J, Claustre H, Aris-Brosou S, Frada M, Not F, de Vargas C (2009) Extreme diversity in noncalcifying haptophytes explains a major pigment paradox in open oceans. Proceedings of the National Academy of Science **106**:12803–12808.

Litchman E, Klausmeier CA, Schofield OM, Falkowski PG (2007) The role of functional traits and trade-offs in structuring phytoplankton communities: scaling from cellular to ecosystem level. Ecology Letters **10**:1170–1181.

Marie D, Partensky F, Jacquet S, Vaulot D (1997) Enumeration and cell cycle analysis of natural populations of marine picoplankton by flow cytometry using the nucleic acid stain SYBR Green I. Applied Environmental Microbiology **63**:186−193.

Martin JH, Gordon RM and Fizwater SE (1991) The case for iron. Limnology and Oceanography **36**:1793-1802.

Mata MM, Wijffels S, Tomczak M, Church JA (2007) Eddy shedding and energy conversions in the East Australian Current. Journal of Geophysical Research **111**: C09034, doi10,1029/2006JC003592.

Matear RJ, Chamberlain MA, Sun C, Feng M (2013) Climate change projection of the Tasman Sea from an Eddy-resolving Ocean Model. Journal of Geophysical Research Oceans 118: 2961–2976.

McCarthy JJ, Goldman JC (1979) Nitrogenous nutrition of marine phytoplankton in nutrient-depleted waters. Science 203:670-672.

McGillicuddy DJ Jr (2016) Mechanisms of physical-biological-biogeochemical interaction at the oceanic mesoscale. Annual Review of Marine Science **8**:13.1–13.36.

McGillicuddy DJ Jr, Robinson AR, Siegel DA, Jannasch HW, Johnson R, et al. (1998) Influence of mesoscale eddies on new production in the Sargasso Sea. Nature **394**:263–265.

Messer LF, Mahaffey C, Robinson C, Jeffries TC, Baker KG, Bibiloni Isaksson J, Ostrowski M, Doblin MA, Brown MV, Seymour JR (2015) High levels of heterogeneity in diazotroph diversity and activity within a putative hotspot for marine nitrogen fixation. The ISME Journal, doi:10.1038/ismej.2015.205.

Milligan AJ, Aparicio UA, Behrenfeld MJ (2012) Fluorescence and nonphotochemical quenching responses to simulated vertical mixing in the marine diatom *Thalassiosira weissflogii*. Marine Ecology Progress Series **448**:67-78.

Moisander PH, Serros T, Paerl RW, Beinart R, Zehr JP (2014) Gammaproteobacterial diazotrophs and nifH gene expression in surface waters of the South Pacific Ocean. The ISME Journal **8**:1962-1973.

Moisander PH, Zhang R, Boyle E, Hewson I, Montoya JP, Zehr JP (2012) Analogous nutrient limitations in unicellular diazotrophs and *Prochlorococcus* in the South Pacific Ocean. The ISME Journal **6**:733–44.

780 Moisander PH, Beinart RA, Hewson I, White AE, Johnson KS, Carlson CA, Montoya JP, Zehr
781 JP (2010) Unicellular cyanobacterial distributions broaden the oceanic N2 fixation domain.
782 Science **327**:1512-1514.

783 Nelson DM, McCarthy JJ, Joyce TM, Ducklow HW (1989) Enhanced near-surface nutrient
784 availability and new production resulting from the frictional decay of a Gulf Stream warm-core
785 ring. Deep-Sea Research A **36**:705–714.

786 Moore CM, Mills MM, Arrigo KR, Berman-Frank I, Bopp L, Boyd PW, Galbraith ED, Geider
787 RJ, Guieu C, Jaccard SL, Jickells RJ, La Roche J et al. (2013) Processes and patterns of oceanic
788 nutrient limitation. Nature Geoscience **6**:701-710.

789 Platt T, Gallegos CL, Harrison WG (1980) Photoinhibition of photosynthesis in natural
790 assemblages of marine phytoplankton. Journal of Marine Research **38**:687-701.

791 Quast C, Pruesse E, Yilmaz P, Gerken J, Schweer T, Yarza P, et al. (2013) The SILVA
792 ribosomal RNA gene database project: improved data processing and web-based tools. Nucleic
793 Acids Research **41**:D590–6.
794 http://www.pubmedcentral.nih.gov/articlerender.fcgi?artid=3531112&tool=pmcentrez&renderty
795 pe=abstract (Accessed November 8, 2013).

796 Ridame C, Le Moal M, Guieu C, Ternon E, Biegala IC, L'Helguen S, et al. (2011) Nutrient
797 control of N_2 fixation in the oligotrophic Mediterranean Sea and the impact of Saharan dust
798 events. Biogeosciences **8**:2773–2783. http://www.biogeosciences.net/8/2773/2011/ (Accessed
799 March 6, 2014).

800 Ridgway K, Godfrey J (1997) Seasonal cycle of the East Australian Current. Journal of
801 Geophysical Research **102**:22,921–22,936.

802 Roughan M, Middleton J (2002) A comparison of observed upwelling mechanisms off the east
803 coast of Australia. Continental Shelf Research 22:2551–2572.

804 Schreiber U (2004) Pulse-Amplitude-Modulation (PAM) fluorometry and saturation pulse
805 method: an overview. In: Papageorgiou G, Govindjee (eds) Chlorophyll a fluorescence: a
806 signature of photosynthesis. Springer. Dordrecht pp 279-319.

807 Seymour JR, Seuront L, Mitchell JG (2007) Microscale gradients of planktonic microbial
808 communities above the sediment surface in a mangrove estuary. Estuarine, Coastal and Shelf
809 Science **73**:651-666.

810 Seymour JR, Doblin MA, Jeffries TC, Brown MV, Newton K, Ralph PJ, Baird M, Mitchell JG
811 (2012) Contrasting microbial assemblages in adjacent water-masses associated with the East
812 Australian Current. Environmental Microbiology Reports **4**:548-555.

813 Turk-Kubo KA, Achilles KM, Serros TRC, Ochiai M, Montoya JP, Zehr JP (2012) Nitrogenase
814 (nifH) gene expression in diazotrophic cyanobacteria in the Tropical North Atlantic in response
815 to nutrient amendments. Frontiers of Microbiology **3**:386-403.

http://www.pubmedcentral.nih.gov/articlerender.fcgi?artid=3487379&tool=pmcentrez&rendertype=abstract (Accessed November 12, 2012).

Uitz J, Huot Y, Bruyant G, Babin M, Claustre H (2008) Relating phytoplankton photophysiological properties to community structure on large scales. Limnology and Oceanography **53**:614-630.

Waite AM, Pesant S, Griffin DA, Thompson PA, Holl CM (2007) Oceanography, primary production and dissolved inorganic nitrogen uptake in two Leeuwin Current eddies. Deep-Sea Research II **54**:981–1002.

Wang Q, Quensen J, Fish J, Lee T, Sun Y, Tiedje J, et al. (2013) Ecological patterns of nifH genes in four terrestrial climatic zones explored with targeted metagenomics using FrameBot, a new informatics tool. MBio 4:e00592–13. http://mbio.asm.org/content/4/5/e00592-13.short (Accessed March 6, 2014).

Wu L, Cai W, Zhang L, Nakamura H, Timmermann A, Joyce T, McPhaden MJ, Alexander M, Qiu B, Visbeck M, Chang P, Giese B (2012) Enhanced warming over the global subtropical western boundary currents. Nature Climate Change **2**:161–166.

Zehr J, Jenkins B, Short S, Steward G (2003) Nitrogenase gene diversity and microbial community structure: a cross system comparison. Environmental Microbiology **5**:539–554. http://onlinelibrary.wiley.com/doi/10.1046/j.1462-2920.2003.00451.x/full (Accessed April 5, 2013).

Zehr J, McReynolds L (1989) Use of degenerate oligonucleotides for amplification of the nifH gene from the marine cyanobacterium *Trichodesmium thiebautii*. Applied Environmental Microbiology **55**:2522–2526.

Zehr J, Turner P (2001) Nitrogen fixation: Nitrogenase genes and gene expression. Methods Microbiology **30**:271–285.

Zehr JP, Mellon MT, Hiorns WD (1997) Phylogeny of cyanobacterial nifH genes: evolutionary implications and potential applications to natural assemblages. Microbiology **143**:1443–1450.

Tables

Table 1: Starting conditions for nutrient amendment experiments in the East Australian Current (EAC) and a cyclonic cold core eddy (CCE). Note that sampling depths targeted the chlorophyll-a fluorescence maximum (Fmax), which was deeper in the EAC than the CCE.

	EAC	**CCE**
Location	29.14817 °S, 154.31495 °E	32.35217 °S, 153.58112 °E
Bottom depth (m)	3279	4632
Sampling depth (Fmax, m)	80	41
Temperature (°C)	21.08	21.31
Salinity	35.52	35.49
Ammonium (µM)	0.07 ± 0.02	0.16 ± 0.01*
Nitrate (µM)	0.26 ± 0.24	0.14 ± 0.02
Phosphate (µM)	0.12 ± 0.02	0.11 ± 0.01
Silicate (µM)	0.84 ± 0.03	0.52 ± 0.01
Total dissolved iron (TDFe) in controls at t72 (nM)	0.38 ± 0.07	1.32 ± 0.23
Chlorophyll-a (µg L^{-1})	0.106 ± 0.008	0.336 ± 0.041

*analytical replicates from same CTD cast, not separate casts as for EAC (n = 2)

Table 2: Effect of experimental manipulation on microbial assemblages in the East Australian Current (EAC) and a cyclonic cold core eddy (CCE) as shown by comparison of t_0 with t_{72} no amendment contol, as well as t_{72} nutrient amendments relative to controls. Treatments include NO_3 (10 µM nitrate final concentration), NO_3+Fe (10 µM nitrate and 1 nM Fe final concentration), Si (10 µM final concentration), and Mix (N+Si+P+Fe; 10N : 10Si : 0.625P µM in Redfield proportions and 1 nM Fe respectively). ++ strong positive difference, P<0.01; + positive difference, P<0.05; --strong negative difference, P<0.01; - negative difference, P<0.05; blank cells: no significant difference; nd: not detected; shaded cells: no measurement.

Parameter	Comparison of t_0 versus t_{72} control		Comparison of t_{72} nutrient amendments versus t_{72} control							
			NO_3		NO_3+Fe		Si		Mix	
	EAC	CCE	EAC	CCE	EAC	CCE	EAC	CCE	EAC	CCE
Chlorophyll a		-	+	+	+	+			+	+
Fucoxanthin:Chl a				+	+	+			+	+
Hex-Fuco:Chl a	-				-	-				
Peridinin:chl a	nd		nd	-	nd	-	nd	-		
Cell abundance*										
- Total pico and nano eukaryote	--	+							--	
- *Prochlorococcus*	--							--		
- *Synechococcus*	+	+							--	--
- Picoeukaryote			--				--		--	
- Nanoeukaryote						+				
- Bacteria								++		++
F_V/F_M			-							
Chl-a fluorescence/cell	--		++	++	++	--		--		--
Phycoerythrin fluorescence/cell			++		++					
Primary production	+		++	++	--	++				
alpha				++		++				
Ik					--	++				
Growth rate										
- Total									-	
- *Prochlorococcus*								--		--
- *Synechococcus*			--						--	
- Picoeukaryote			--				--		--	
- Nanoeukaryote						+				
- Bacteria								++		++

*Estimated from flow cytometry

862 **Figures**

863

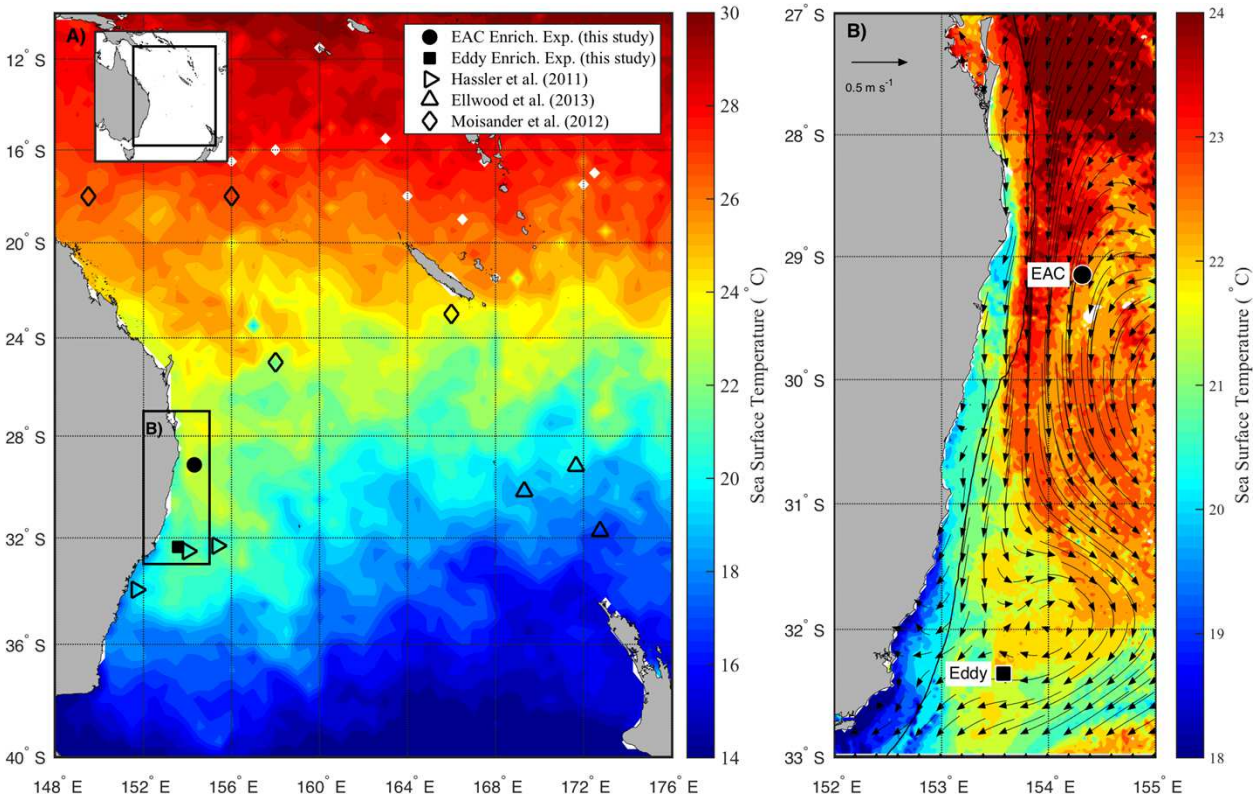

864

865 1. **Study area.** (A) Average sea surface temperature (SST) for October 2010 in the Tasman
866 Sea, eastern Australia. The location of previous nutrient amendment studies are shown
867 with symbols. The black box is the domain for the current study. (B) Average SST (20-
868 25th October 2010) of the study domain during the voyage, showing location of sampling
869 sites. The black line shows 200 m isobath, which approximates the continental shelf edge.
870 Geostrophic velocities, estimated from sea-level anomaly are shown as arrows (20th
871 October 2010).

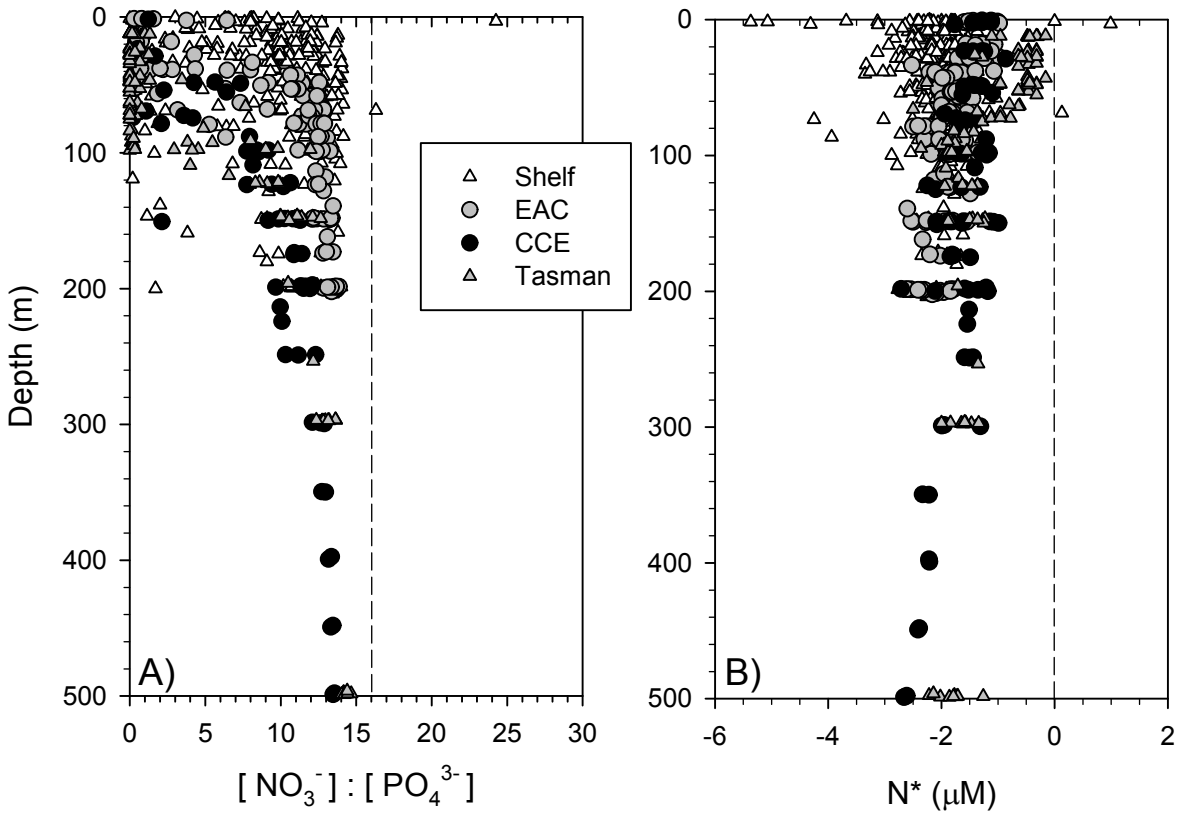

2. **Dissolved nitrogen pool relative to phosphorus.** The ratio of dissolved nitrate and phosphate (A) and nitrate deficit ($N^* = [NO_3^-] - 16[PO_4^{3-}]$) (B) in waters of the study domain, including the continental shelf (white triangles), East Australian Current (EAC; grey circles), cyclonic cold-core eddy (CCE; black circles) and Tasman Sea (grey triangles).

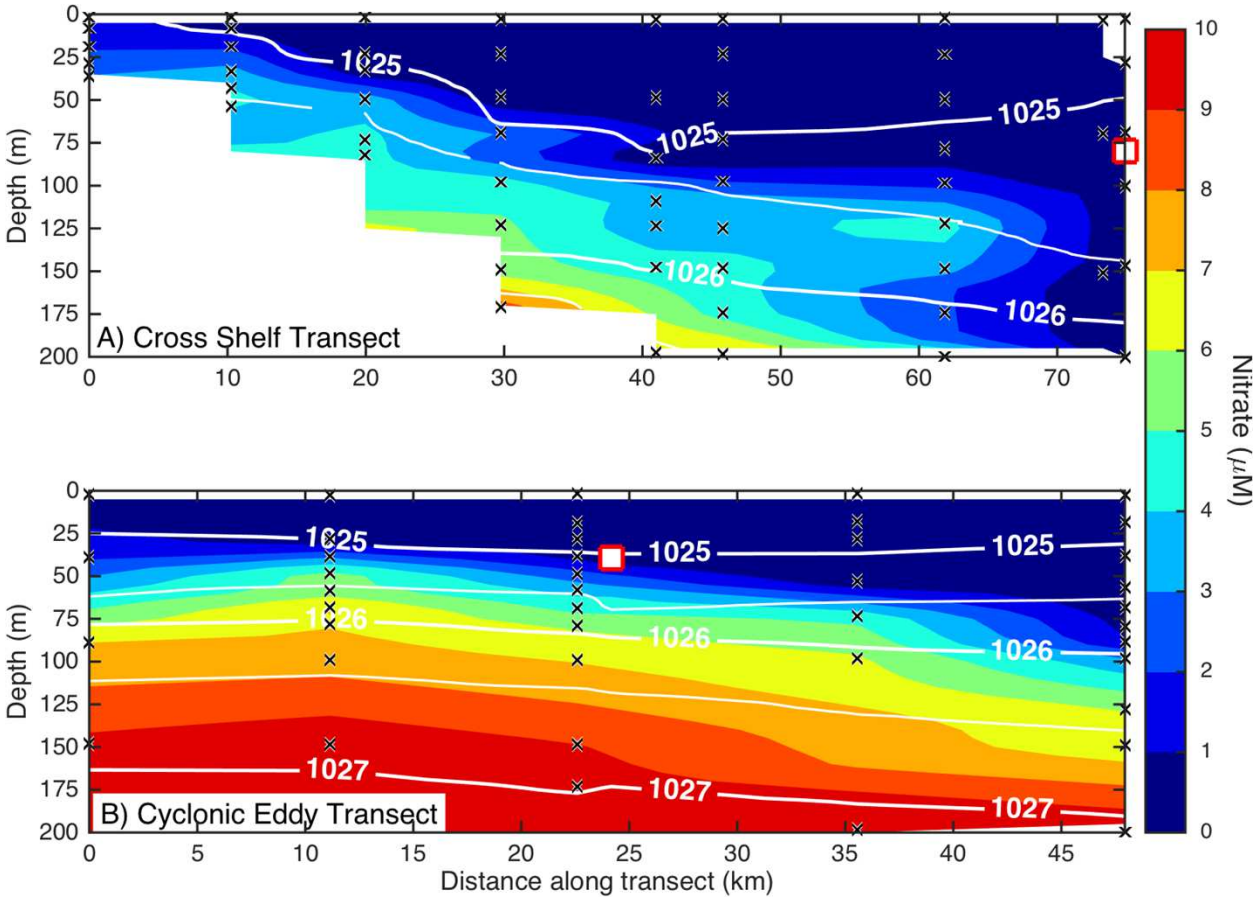

3. **Eddy influence on vertical nutrient distribution.** The distribution of dissolved nitrate (A) across the continental shelf to the East Australian Current, and (B) across the sampled cyclonic cold-core eddy. The white contours indicate seawater density, and the black crosses show the sampling locations for nitrate. The white squares indicate the water sampling locations for the nutrient amendment experiments.

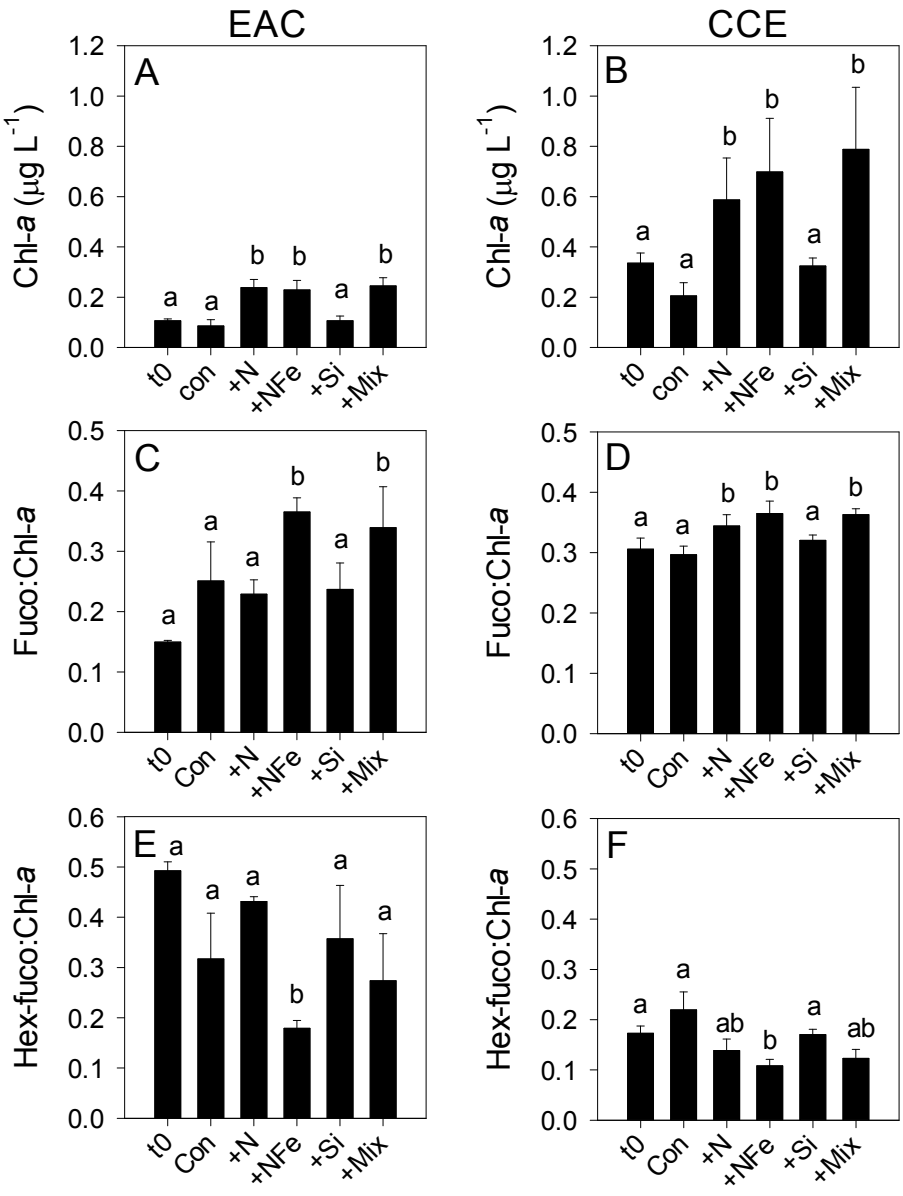

4. **Phototrophic responses to nutrient amendment.** Total Chl-a (monovinyl + divinyl), ratio of fucoxanthin to Chl-a and ratio of hex-fucoxanthin to Chl-a in the EAC (A, C and E, respecively) and CCE (B, D and F, respectively). These parameters are proxies for total phytoplankton biomass (Chl-a), relative biomass of diatoms (Fuco:Chl-a) and relative biomass of haptophytes (Hex-fuco:Chl-a). Treatments include initial (t0) and after 3 days nutrient amendment: Con = control, no amendment; +N = nitrate; +NFe = nitrate + iron; +Si = silicate; +Mix = nitrate + phosphate + silicate + iron. Values plotted are mean ± standard deviation. Letters above bars indicate statistical differences amongst treatments (ANOVA, $\alpha = 0.05$) such that a is different to b, and ab is the same as a and b.

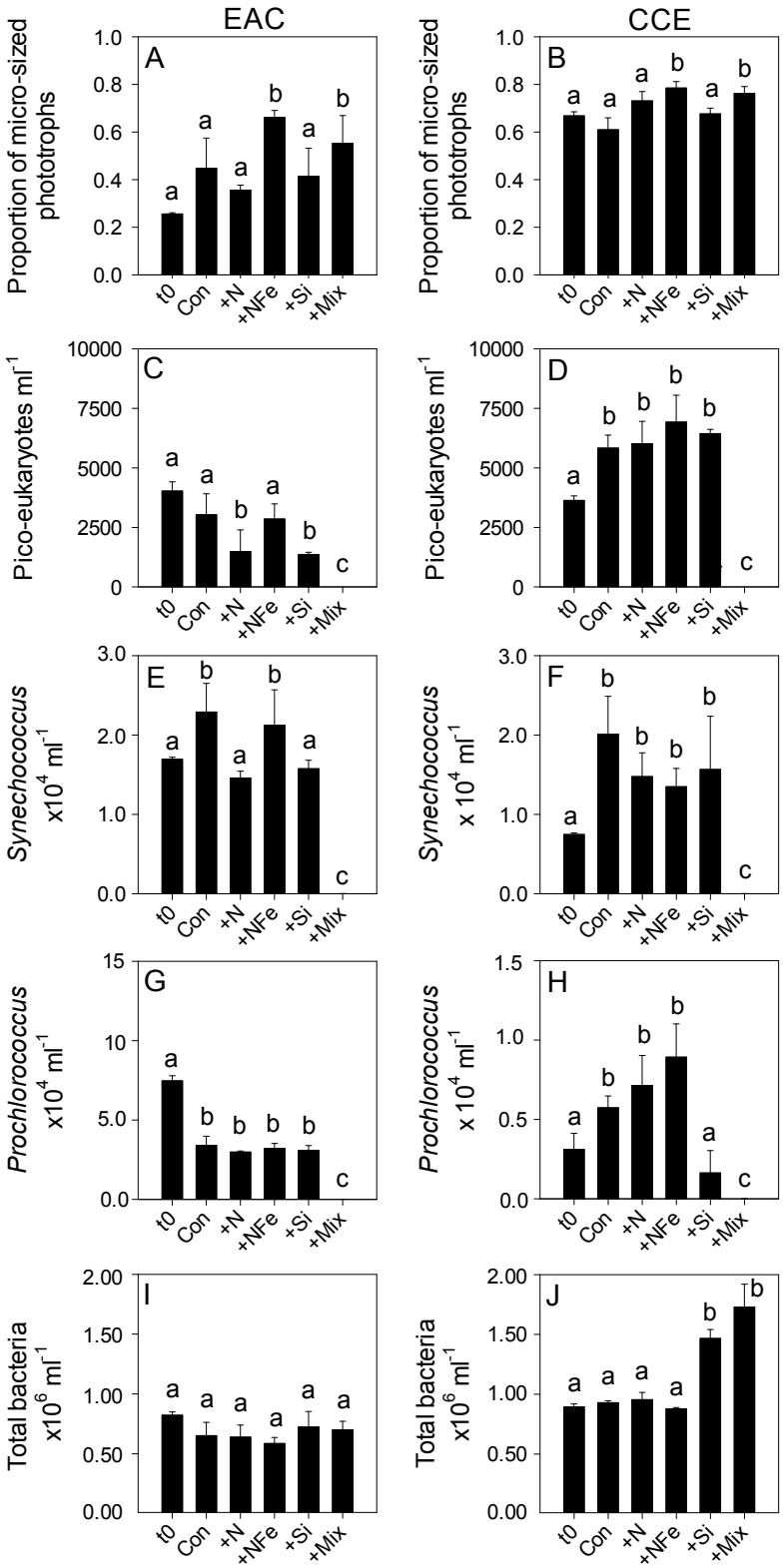

903
904

5. **Phototrophic and total bacteria responses to nutrient amendment.** Proportion of phototrophs larger than 20 µm in the EAC (A) and CCE (B), abundance of picoeukaryotes (C and D), abundance of *Synechococcus* (E and F), abundance of *Prochlorococcus* (G and H), and abundance of total bacteria (I and J). Treatments as in Figure 4. Values plotted are mean ± standard deviation. Letters above bars indicate statistical differences amongst treatments (ANOVA, $\alpha = 0.05$) such that a is different to b and c.

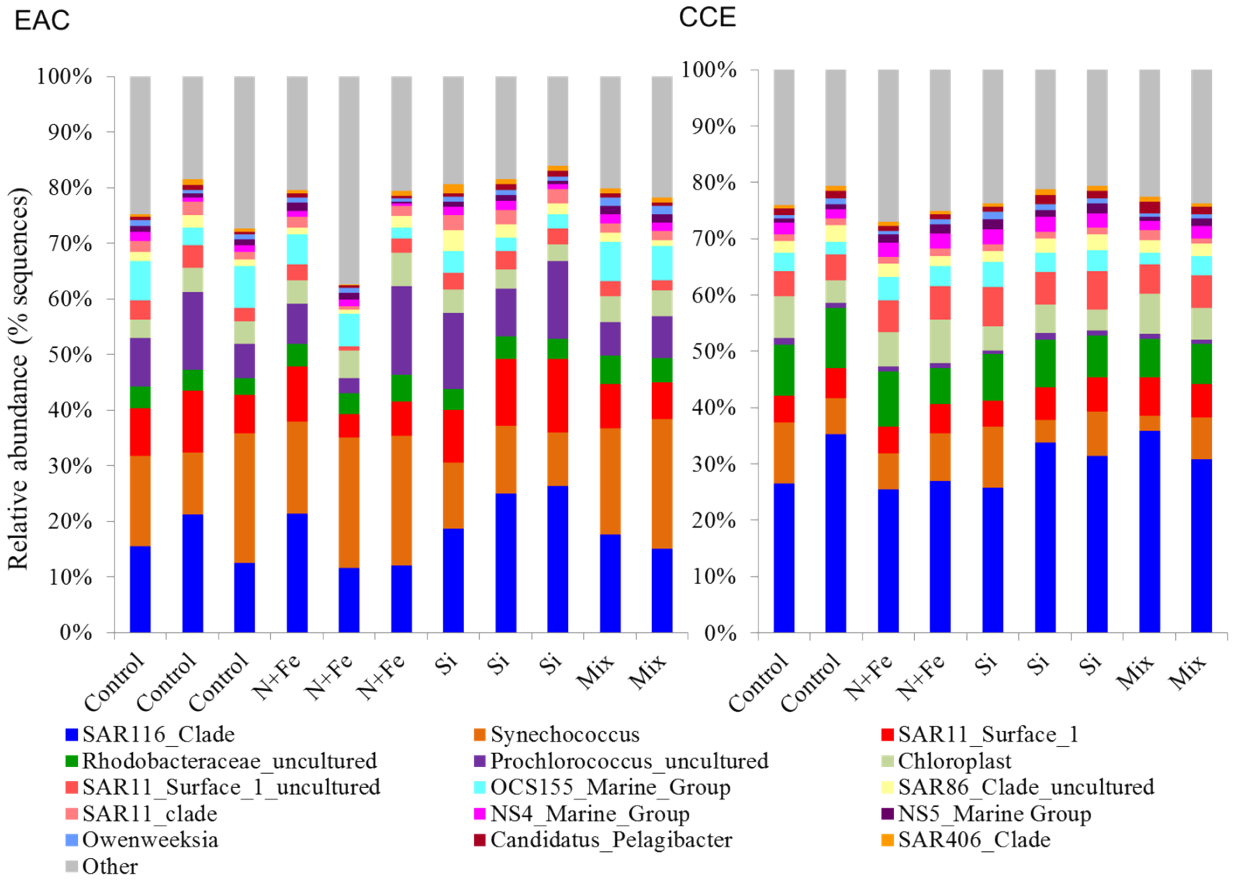

6. **Relative abundance of 16S rRNA operational taxonomic units**. Data are shown for sequences with ≥ 97 % sequence similarity to the SILVA database in the EAC (A) and CCE (B) amongst different treatments. For visual simplicity, only the top 15 OTUs are presented, with the upper grey bars representing the remaining 16S sequences detected. Control = no amendment; N+Fe = addition of nitrate and iron (10 µM and 1 nM, respectively), Si = addition of silicate (10 µM) and Mix = addition of nitrate, phosphate, silicate and iron (10 µM, 0.625 µM, 10 µM, 1 nM, respectively).

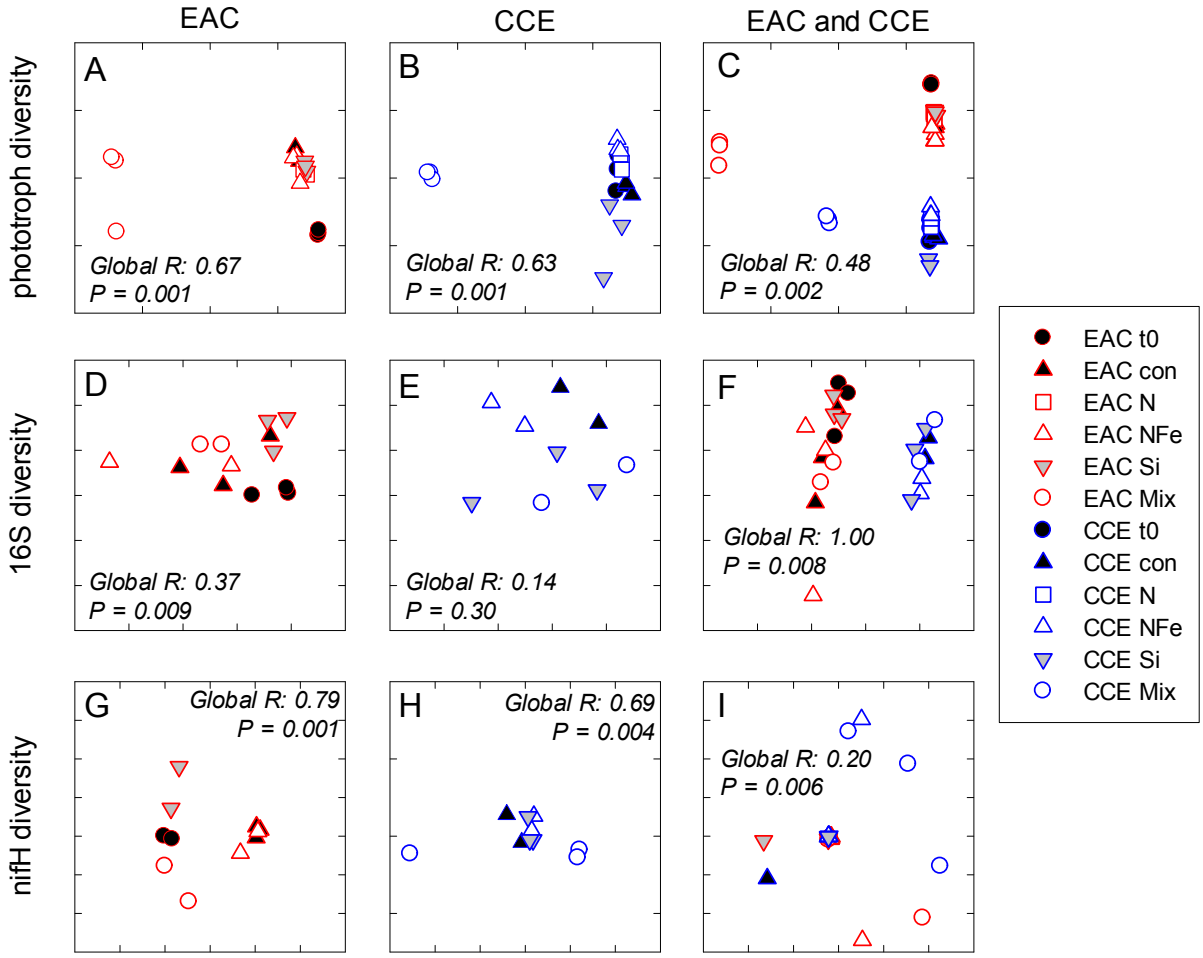

7. Diversity of microbial communities. Multi-dimensional Scaling (MDS) plots of phototrophs (A,B and C), bacteria (D, E and F) and diazotrophs (G, H and I) in the East Australian Current (EAC), cyclonic (cold-core) eddy (CCE) and both the EAC and CCE. Clustering of samples is based on a Bray-Curtis similarity matrix of square-root transformed HPLC pigment concentrations and flow cytometric counts of phototroph abundance, Operational Taxonomic Units from 16S ribosomal genes or nitrogenase *NifH* subunit genes. Plots on the same row have the same axes scales, to make them directly comparable. Stress values for all plots are <0.10.

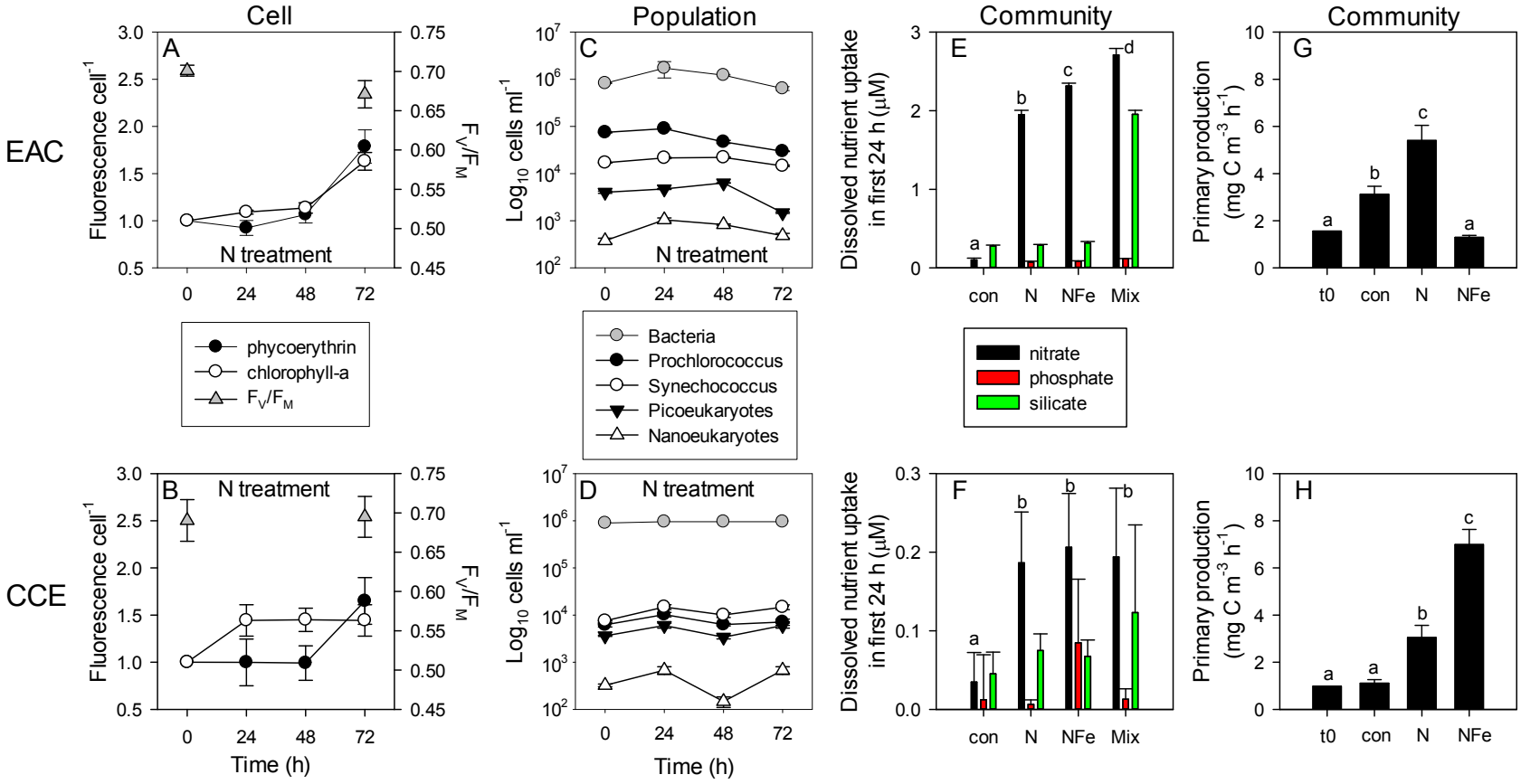

8. **Time-course of microbial responses to nutrient addition.** Daily Chl-a and phycoerythrin fluorescence in small pico-eukaryotes and *Synechococcus*, respectively under N amendment (A and B), together with photosynthetic efficiency (F_V/F_M) of the control phytoplankton assemblage at t_0 and t_{72}; Daily abundance of phototrophic and bacterial populations (C and D) in +N treatments in the EAC and CCE; Rate of macro-nutrient uptake in the first 24 h of incubation (E and F); Total carbon fixation by the phytoplankton assemblage in different treatments on day 3 (G and H). Values plotted are mean ± SD (n = 3) except for plots C and D which are mean ± SE (n = 3). Letters above bars indicate statistical differences amongst treatments (ANOVA, $\alpha = 0.05$) such that a is different to b, c and d.

945